

## 12. SITE 563<sup>1</sup>

### Shipboard Scientific Party<sup>2</sup>

#### HOLE 563

**Date occupied:** 24 October 1981

**Date departed:** 28 October 1981

**Time on hole:** 77 hr.

**Position (latitude; longitude):** 33°38.53'N; 43°46.04'W

**Water depth (sea level; corrected m, echo-sounding):** 3786

**Water depth (rig floor; corrected m, echo-sounding):** 3796

**Bottom felt (m, drill pipe):** 3796

**Penetration (m):** 382.5

**Number of cores:** 25

**Total length of cored section (m):** 226

**Total core recovered (m):** 190.6

**Core recovery (%):** 84

**Oldest sediment cored:**

Depth sub-bottom (m): 364.5

Nature: Limestone

Age: early Oligocene

**Basement:**

Depth sub-bottom (m): 364.5

Nature: Basalt

**Principal results:** Hole 563 (MAR-11) was drilled on Anomaly 13 on the west flank of the Mid-Atlantic Ridge about 60 mi. south of Hayes Fracture Zone (Fig. 1).

The sediments were washed down to 156.5 m and then rotary cored down to 364 m where the basement was felt. The entire recovered section of sediment consists of calcareous pelagic ooze. Two sediment units, similar to those at Site 558, are recognized and their boundary occurs roughly at the same age level as at Site 558. The sediment accumulation rates of each unit are similar to those of Site 558. However, the lithologic differences between the two units are more distinct at Site 558 than at Site 563.

The basement was only cored for 18.5 m because of difficult drilling conditions and premature bit failure. The recovered sam-

ples consist of one petrographic unit of sparsely plagioclase phyr-ic basalts presenting a depleted character ( $Nb = 1.7$  ppm,  $Zr = 55$  ppm,  $(Nb/Zr)_{ch} = 0.3$ ).

No downhole measurements were taken at this site.

#### OPERATIONS

##### Approach to Site

From Site 562, the *Challenger* headed northwest along a flow line toward Site MAR-11 located on Anomaly 13 south of the Hayes Fracture Zone. Around 0100Z, 25 October (Fig. 2), the *Challenger* crossed a buried basement ridge that had several potential sites. In particular, a site crossed at 0108Z (Fig. 3) had the right combination of relatively smooth basement and less than 0.4 s of sediments. At 0122Z the *Challenger* reversed course and the beacon was dropped on Site 563 at 0152Z.

##### On-Site Operations

Hole 563 was spudded at 1000Z, 25 October, in 3796 m of water. The sediments were washed to a depth of 156.5 m sub-bottom, where continuous rotary coring was started. Between 1330Z, 25 October and 1852Z, 26 October, 22 sediment cores were recovered (Table 1). Hard rock was hit at a depth of 364 m sub-bottom. Drilling within basement was extremely slow; it took 10 hr. to cut Core 25. While we were trying to retrieve Core 25, the drill string became stuck, the drill bit released prematurely, and the core barrel fell out. The core barrel was eventually recovered, but the hole had to be abandoned. We decided to continue drilling at Site MAR-11 at a site approximately 5 or 10 mi. away. The drill string was pulled, and the *Challenger* was underway to Site 564 at 0530Z, 28 October.

#### LITHOLOGY

Rotary coring in Hole 563 (water depth 3630 m) was begun after 156.5 m were washed down and one wash core was retrieved. The stratigraphic position of Core 563-1 is very close to that of Core 588-1 (lower upper Miocene). The sedimentary section was cored continuously from 156.5 m down to lower Oligocene basement at 364.5 m, so that a section very similar to that in Hole 558 was recovered (Fig. 4). Plans to recover the younger section from 0 to 156.5 m with the hydraulic piston corer had to be aborted when the bit and core barrel were lost in the hole during the cutting of the third basalt core. We then decided to move to another site and wash down to basement.

Based on differences in color, small differences in carbonate content, and changes in lithification and sediment accumulation rates (Fig. 5), we could recognize

<sup>1</sup> Bougault, H., Cande, S. C., et al., *Init. Repts. DSDP*, 82: Washington (U.S. Govt. Printing Office).

<sup>2</sup> Henri Bougault (Co-Chief Scientist), IFREMER (formerly CNEXO), Centre de Brest, B.P. 337, 29273 Brest Cedex, France; Steven C. Cande (Co-Chief Scientist), Lamont-Doherty Geological Observatory, Columbia University, Palisades, New York; Joyce Brannon, Department of Earth and Planetary Sciences, Washington University, St. Louis, Missouri; David M. Christie, Hawaii Institute of Geophysics, University of Hawaii at Manoa, Honolulu, Hawaii; Murlene Clark, Department of Geology, Florida State University, Tallahassee, Florida; Doris M. Curtis, Curtis and Echols, Geological Consultants, Houston, Texas; Natalie Drake, Department of Geology, University of Massachusetts, Amherst, Massachusetts; Dorothy Echols, Department of Earth and Planetary Sciences, Washington University, St. Louis, Missouri (present address: Curtis and Echols, Geological Consultants, 800 Anderson, Houston, Texas 77401); Ian Ashley Hill, Department of Geology, University of Leicester, Leicester LE1 7RH, United Kingdom; M. Javed Khan, Lamont-Doherty Geological Observatory, Columbia University, Palisades, New York (present address: Department of Geology, Peshawar University, Peshawar, Pakistan); William Mills, Deep Sea Drilling Project, Scripps Institution of Oceanography, La Jolla, California (present address: Ocean Drilling Program, Texas A&M University, College Station, Texas 77843); Rolf Neuser, Institut für Geologie, Ruhr Universität Bochum, 4630 Bochum 1, Federal Republic of Germany; Marion Rideout, Graduate School of Oceanography, University of Rhode Island, Kingston, Rhode Island (present address: Department of Geology, Rice University, P.O. Box 1892, Houston, Texas 77251); and Barry L. Weaver, Department of Geology, University of Leicester, Leicester, LE1 7RH, United Kingdom (present address: School of Geology and Geophysics, University of Oklahoma, Norman, Oklahoma 73019).

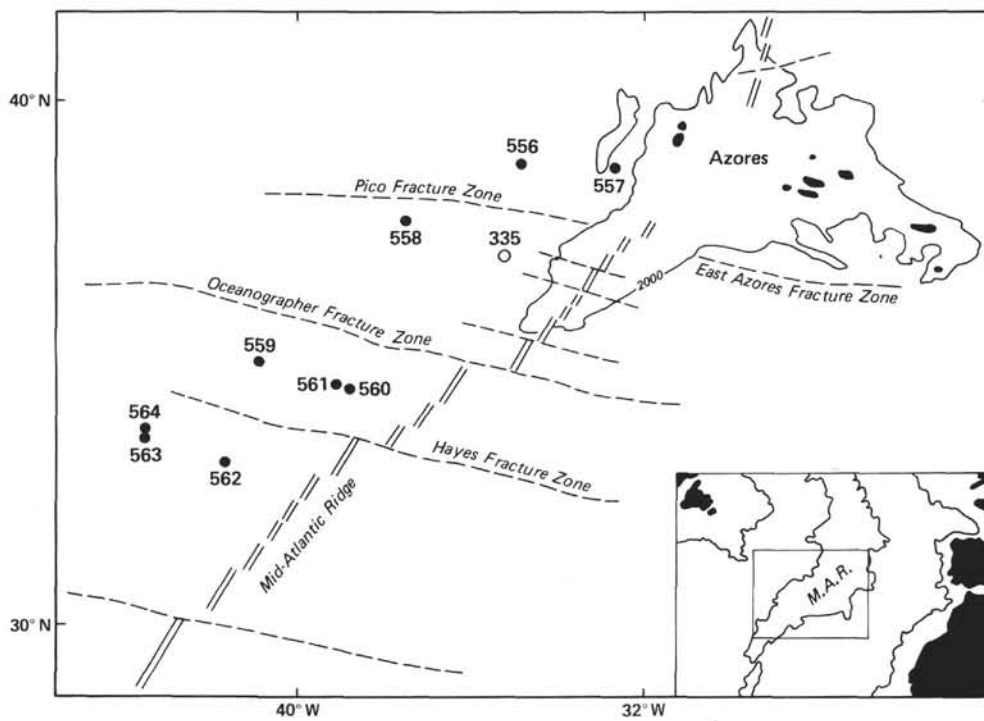


Figure 1. Site location map, Leg 82.

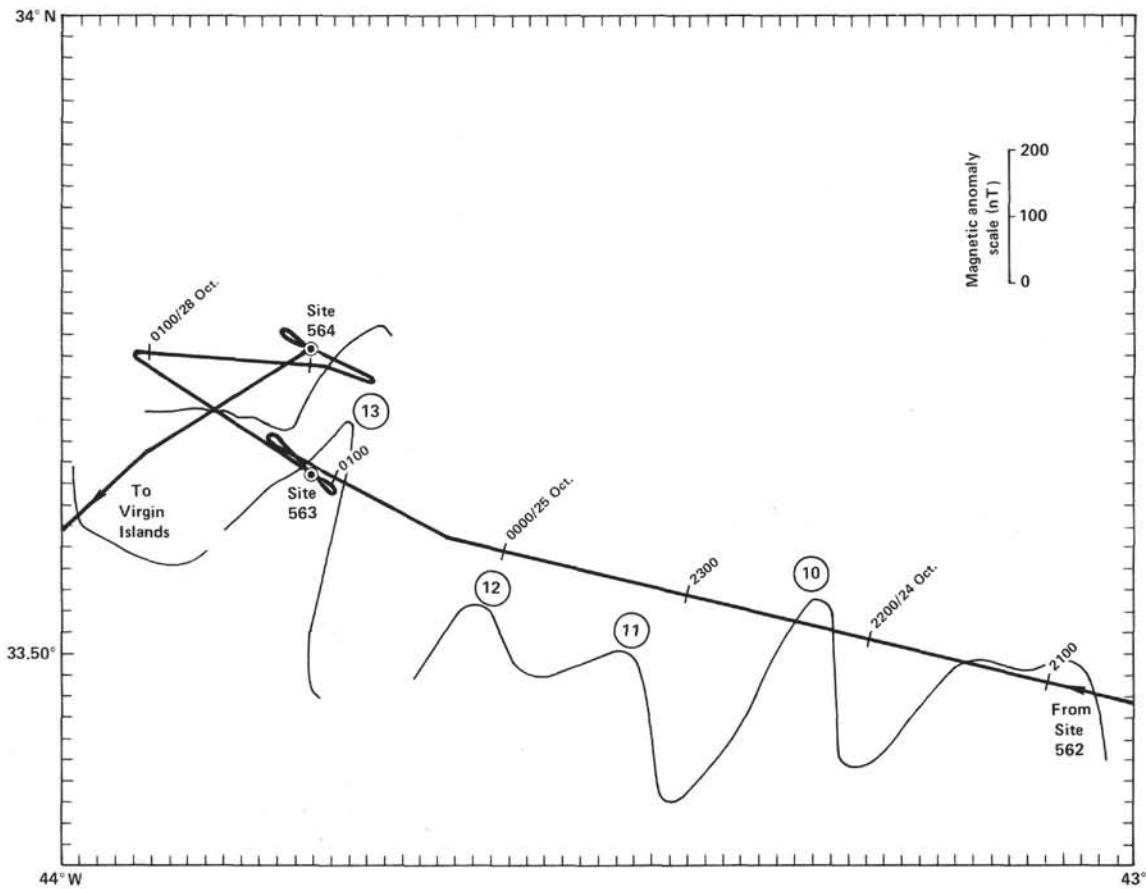


Figure 2. Approach and site survey tracks for Sites 563 and 564. Heavy line is the ship's track with hours marked in GMT. Thin line is the magnetic anomaly projected perpendicularly from ship's track. Circled numbers are anomalies based on work at Lamont-Doherty Geological Observatory.

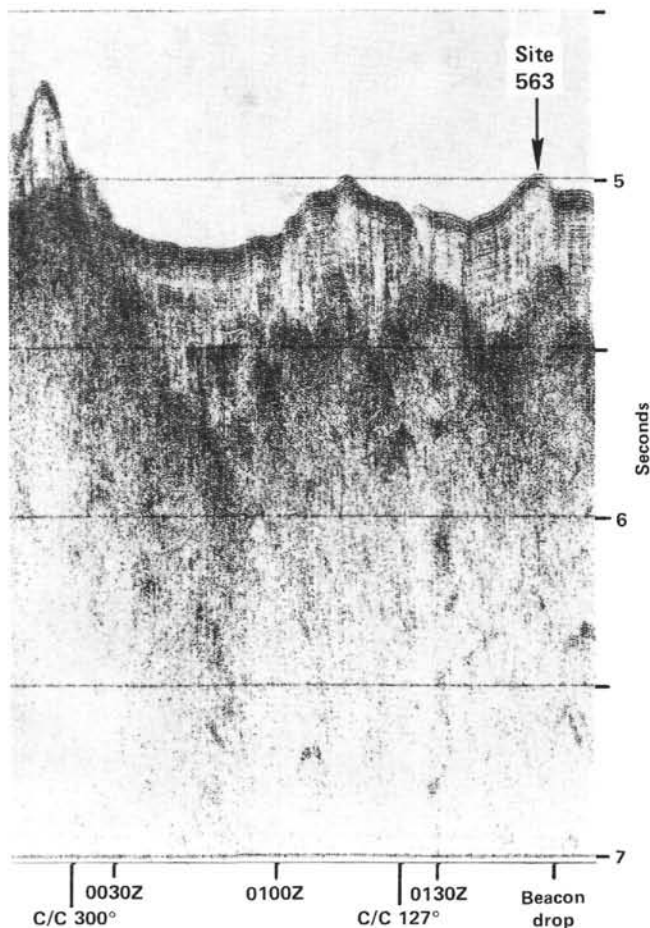


Figure 3. *Glomar Challenger* seismic profile of the approach to Site 563. C/C = course change. For location of profile, see Figure 2.

Table 1. Coring summary, Hole 563.

Core	Date (Oct. 1981)	Time (Z)	Depth from drill floor (m)	Depth below seafloor (m)	Length cored (m)	Length recovered (m)	Percent recovered
H1	25	1330	3796.0-3952.5	0.0-156.5	0.0	0.00	0
1	25	1508	3952.5-3962.0	156.5-166.0	9.5	4.52	48
2	25	1607	3962.0-3971.5	166.0-175.5	9.5	9.62	100+
3	25	1730	3971.5-3981.0	175.5-185.0	9.5	9.02	95
4	25	1845	3981.0-3990.5	185.0-194.5	9.5	5.01	53
5	25	2030	3990.5-4000.0	194.5-204.0	9.5	9.70	100+
6	25	2140	4000.0-4009.5	204.0-213.5	9.5	9.51	100+
7	25	2310	4009.5-4019.0	213.5-223.0	9.5	9.63	100+
8	26	0025	4019.0-4028.5	223.0-232.5	9.5	9.31	98
9	26	0150	4028.5-4038.0	232.5-242.0	9.5	9.58	100+
10	26	0300	4038.0-4047.5	242.0-251.5	9.5	9.63	100+
11	26	0405	4047.5-4057.0	251.5-261.0	9.5	6.31	66
12	26	0522	4057.0-4066.5	261.0-270.5	9.5	9.50	100
13	26	0714	4066.5-4076.0	270.5-280.0	9.5	7.47	79
14	26	0830	4076.0-4085.5	280.0-289.5	9.5	9.50	100
15	26	0942	4085.5-4095.0	289.5-299.0	9.5	9.48	99
16	26	1107	4095.0-4104.5	299.0-308.5	9.5	9.60	100+
17	26	1215	4104.5-4114.0	308.5-318.0	9.5	9.56	100+
18	26	1330	4114.0-4123.5	318.0-327.5	9.5	6.85	72
19	26	1450	4123.5-4133.0	327.5-337.0	9.5	3.66	39
20	26	1610	4133.0-4142.5	337.0-346.5	9.5	9.66	100+
21	26	1731	4142.5-4151.5	346.5-355.5	9.0	9.63	100+
22	26	1852	4151.5-4160.5	355.5-364.5	9.0	4.79	53
23	26	2318	4160.5-4169.5	364.5-373.5	2.0	1.20	60
24	27	0623	4162.5-4169.5	366.5-373.5	7.0	4.87	70
25	27	2115	4169.5-4178.5	373.5-382.5	9.0	2.95	33
					226.0	190.56	84

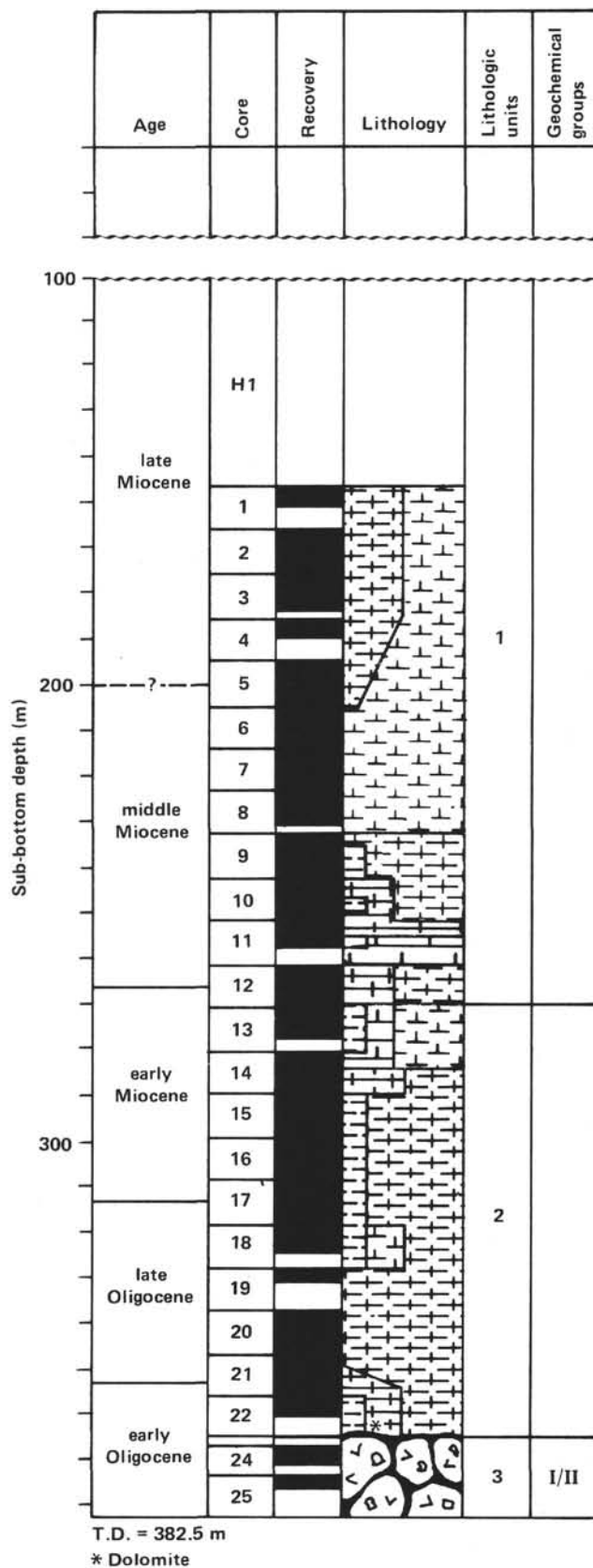


Figure 4. Lithology column, Hole 563. Water depth is 3796.0 m. T.D. is total depth. Asterisk indicates dolomite. For lithologic symbols, see Explanatory Notes chapter, this volume.

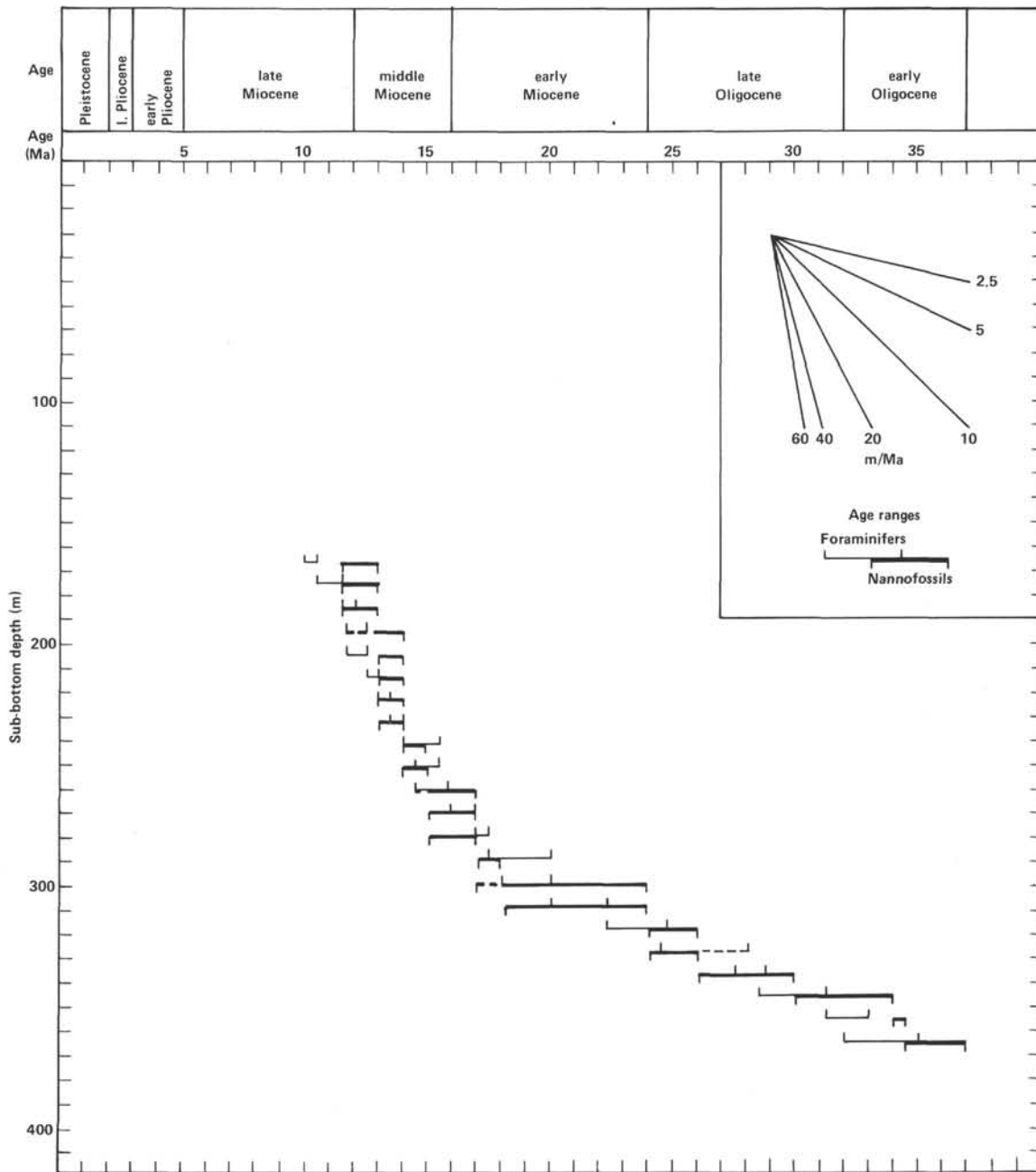


Figure 5. Sediment accumulation rates, Hole 563.

two units at this site. Unit 1 is a white to pale brown to yellowish brown ooze and chalk, of the middle to late Miocene, with an average sediment accumulation rate of 20 m/Ma. Unit 2 is a darker, pale brown to brown to yellowish brown, more-or-less clayey calcareous pelagic chalk and ooze of the early Miocene and Oligocene, with an average sediment accumulation rate of 5 m/Ma. We have summarized the sediment lithology of these two units in Table 2 and have described them in order of their depositional sequence beginning with Unit 2.

**Unit 2**

Open-ocean calcareous pelagic sedimentation began at this site immediately after the formation of the early

Oligocene (34–37 Ma) ocean crust and continued throughout the Cenozoic. Lithologic Unit 2 of Hole 563 consists of 94 m of pelagic ooze and chalk deposited during the interval from the early Oligocene (34–37 Ma) through early Miocene (15–17 Ma). This unit extends from Core 22 (plus a 3-cm piece of limestone at the top of Core 23) up through Core 13. Throughout the unit, lithification alternates between chalk and ooze. Chalk is a dominant component only in Cores 21 and 22.

At the base of the sediment section is approximately 18 m (Core 563-22 and Sections 563-21-2 to 563-21-7) of dolomitic clayey chalk/ooze (Core 22) and dolomite-bearing chalk/ooze (Core 21), containing varying proportions of foraminifers and nannofossils. These lower

Table 2. Sediment lithology summary, Hole 563.

Interval	Unit designation	Depth interval (thickness) (m)	Main colors	Main lithology	Main components	Structure	Age
563-1-1 to 563-12, CC	1	156.5-270.5 (114.0)	White to pale brown	Foraminiferal-nannofossil ooze and chalk; nannofossil ooze	Nannofossils, foraminifers	Uniform with minor to moderate mottling	late/middle Miocene to middle/early Miocene
563-13-1 to 563-23-1, 3 cm	2	270.5-364.5 (94.0)	Pale brown to brown	Foraminiferal-nannofossil ooze and chalk; nannofossil ooze and chalk; clayey foraminiferal-nannofossil chalk and ooze	Nannofossils, foraminifers, clay	Uniform with minor mottling	middle/early Miocene to early Oligocene

Oligocene sediments are brown (10YR 5/3), massively bedded, and only very mildly bioturbated. They contain 87–92% carbonate (see Fig. 6), and their primary constituents are nannofossils (56–69%), foraminifers (5–24%), clay (7–15%), and authigenic dolomite rhombs (2–10%). The dolomite rhombs decrease from Core 563-22 up to Section 563-21-2, and then occur in trace quantities in Cores 20, 19, 14, 11, and 10. Zeolites are present in trace quantities except where we have estimated 1–5% (in Sections 563-21-3 and 563-21-4). Micronodules are present in trace quantities.

The greater part (80 m) of the sediments in Unit 2 (Section 563-21-1 up through Core 563-13; upper Oligocene through lower Miocene) consists of calcareous ooze/chalk and clayey calcareous ooze/chalk, with varying proportions of foraminifers and nannofossils. These beds are generally yellowish brown (10YR 5/4) and pale brown (10YR 6/3). Color changes are gradational and indistinct; hard layers are generally darker. The sediments are massively bedded. Bioturbation is minor to absent in Cores 21 through 17 and increases in Cores 16 through 13. Halo burrows are present in Cores 15 through 13. Average carbonate content is between 80 and 90%. The dominant sediment components are nannofossils (54–84%, but generally in the 60–70% range) and foraminifers, whose abundance is highly variable (5–25%, but generally more than 10%). Estimated clay content varies between 5 and 17%, but amounts less than 10% are found only in Cores 14 and 20. Zeolites occur in Cores 15 through 20 in quantities estimated between 1 and 5%. Micronodules are present in trace quantities, except for an estimated 2% in Core 18. Lithification alternates between ooze and chalk, but ooze is dominant in this interval.

The sediments in Cores 12 through 10, which we have assigned to Unit 1, have similar lithology but are transitional in composition, color, and lithification. Because of the similarity of their position in the lithologic sequence and their age, when compared to the sediments of Hole 558, we have placed these cores in Lithologic Unit 1.

### Unit 1

Open-ocean calcareous pelagic sedimentation continued during the deposition of Unit 1 at Hole 563. The cored portion of the unit consists of 114 m (Cores 12 through 1) of pelagic ooze and chalk deposited during middle Miocene and early late Miocene times (10–13 to 15–17 Ma). Deposition of the unit began with a sequence transitional from Unit 2 that crosses the boundary between the lower and middle Miocene sections. This transitional sequence consists of 28.5 m of nannofossil and foraminiferal-nannofossil chalk/ooze, with a few clayey intervals. Colors alternate from very pale brown (10YR 7/3) to pale brown (10YR 6/3) to yellowish brown (10YR 5/4) with indistinct gradational contacts between the colors. Bedding is massive, and bioturbation is moderate; large halo burrows are common. Carbonate content is between 86 and 96%. The dominant sediment component (see Fig. 6) in the transitional sequence is nannofossils (66–84%), followed by foraminifers (2–25%, but mostly more than 10%), and clay (5–14%, but generally less than 10%). Manganese nodules 1 to 4 mm in diameter are present, as well as micronodules in trace amounts. Lithification alternates between ooze and chalk, but chalk predominates.

Above the transition zone, in Cores 9 through 1, the section consists of foraminiferal-nannofossil ooze and nannofossil ooze, with a few intervals of slightly clayey ooze. The dominant color is white grading with subtle color changes from mostly white (10YR 8/1–8/2) to light gray (10YR 7/1) and very pale brown (10YR 7/4 and 10YR 8/3), with the darker shades toward the bottom of Core 9. Mottling and bioturbation are minor to moderate, with more bioturbation in the darker intervals, especially in Core 9. Bedding is massive, but indistinct color banding may be related to bedding. Carbonate content is 87–97%; most values in the sediments above Core 9 are more than 90%. The principal sediment components are nannofossils, which vary in abundance between 69 and 93%. Foraminiferal abundances range between 1 and 15%; foraminifers appear to be more abun-

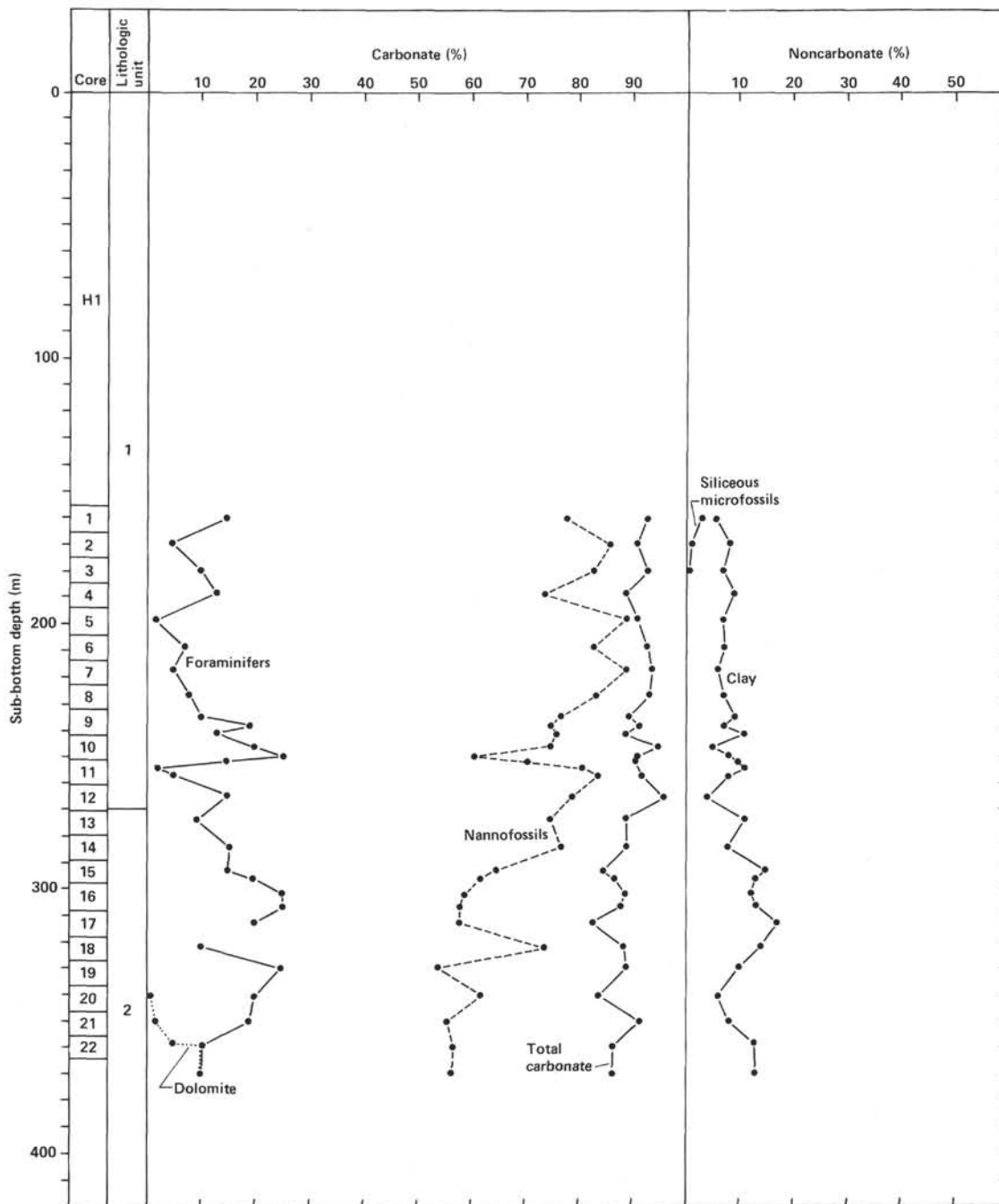


Figure 6. Percentage plot of major sediment components, Hole 563.

dant in Cores 1 through 5. Clay content is generally below 10%, except in short intervals in Core 4.

**BIOSTRATIGRAPHY**

Hole 563 was washed down to 156.5 m where 22 rotary sediment cores were taken above basement. Sediment was not obtained from Core 23, which reached basalt; consequently, the oldest part of the section was not recovered. Although hydraulic piston coring program was scheduled for this site to retrieve sediment from the top 156.5 m of the section, this part of the program was cancelled because of drilling problems.

Sediment recovered at this site is assigned to the lower upper Miocene to lower Oligocene based on data from calcareous nannofossils. Assignments based on planktonic foraminifers are upper Miocene to lower Oligocene. No hiatuses in the cored section are apparent; all major nannofossil zones of Okada and Bukry (1980) for this interval are recognized.

Calcareous nannofossils are abundant, and planktonic foraminifers are common to abundant throughout the section. Preservation in both microfossil groups ranges from good to moderate. Increased planktonic foraminiferal fragmentation is noted in the Miocene sections,

which seems to indicate that increased dissolution occurred during the Miocene. Nannofossils are less well preserved in the lower Miocene and Oligocene sections.

Benthic foraminifers and ostracodes are diverse and well preserved throughout the section. Benthic foraminifers range in abundance from common to few.

Figure 7 shows the correlation of the foraminiferal and nannofossil zones encountered on Leg 82 (Holes 558, 558A, and 563) with Hole 334 drilled on Leg 37 (Aumento, Melson, et al., 1977). The lower upper Miocene section retrieved in Hole 334 approximates the intervals missing from sections cored on Leg 82; therefore we have a more complete sedimentary section than has previously been recovered from the Cenozoic of the mid-Atlantic between 20 and 40°N latitude.

### Calcareous Nannofossils

Cores 1 through 3 contain *Discoaster hamatus* and are assigned to the *D. hamatus* Zone CN7 (NN9), which is upper middle to lower upper Miocene. Cores 2 and 3 contain common *Catinaster calyculus*, which may indicate the upper portion of the *Discoaster hamatus* Zone (Okada and Bukry, 1980).

The top of Core 4 (563-4-1, 80 cm) contains *C. coalitus* without *D. hamatus* and represents the rather short *C. coalitus* Zone CN6 (NN8), which is middle Miocene.

The interval from 563-4,CC through 563-8,CC is placed in the middle Miocene *D. exilis* Zone CN5 (NN6-NN7). This zone represents the interval between the first appearance of *D. hamatus* and the last appearance of *Sphenolithus heteromorphus*.

A lower middle Miocene CN4 (NN5) assignment is indicated for Cores 9 and 10 by the coexistence of *S. heteromorphus* and long-armed discoasters. Cores 11 through 12 contain *S. heteromorphus*, but the long-armed discoasters are rare to absent, suggesting that this interval belongs to the *Helicosphaera ampliapertura* Zone CN3 (NN3-NN4). *H. ampliapertura*, whose last occurrence marks the boundary between the *Sphenolithus heteromorphus* Zone and the *Helicosphaera ampliapertura* Zone, was not found at this site. The first appearance of long-armed discoasters must therefore be used to distinguish the two zones.

Because of the presence of *Sphenolithus belemnos* and *S. heteromorphus*, 563-12,CC is placed in the *S. belemnos* Zone CN2 (NN2-NN3) and is lower Miocene. The core catcher of Core 14 is also assigned to this zone.

The Oligocene/Miocene boundary is located within the *Triquetrorhabdulus carinatus* Zone CN1 (NN1-NP25) represented by Cores 15 and 16. The characteristic species for this interval are *T. carinatus*, *Cyclicargolithus floridanus*, and *Discoaster deflandrei*.

An upper Oligocene assignment is suggested for Cores 17 and 18 by the presence of *Sphenolithus ciperoensis*. *S. ciperoensis* is the index species for the *S. ciperoensis* Zone CP19 (NP24-NP25). Core 19 contains *S. distentus* without *S. ciperoensis* and is placed in the upper Oligocene *S. distentus* Zone CP18 (NP23).

The core catcher of Core 20 represents the interval between the last appearance of *Reticulofenestra umbilica*

and the first appearance of *Sphenolithus distentus*. This sample is assigned to the *S. predistentus* Zone CP17 (NP23) and is lower Oligocene.

The core catcher of Core 21 contains *Reticulofenestra umbilica* without *Coccolithus formosus* and is placed in the *Helicosphaera reticulata* Zone, *Reticulofenestra hillaie* Subzone CP16c (NP22). *R. umbilica* occurs with *Coccolithus formosus* in 563-22,CC, indicating that this sample should be assigned to the lower Oligocene *Coccolithus formosus* Subzone CN16b (NP21) of the *Helicosphaera ampliapertura* Zone.

*Braarudosphaera rosa* commonly occurs in Cores 20 through 22. The Oligocene presence of these species in the North Atlantic may in some way be environmentally related to the middle-Oligocene *Braarudosphaera* chalks in the South Atlantic.

### Foraminifers

#### Miocene (upper)

Upper Miocene sediments were recovered in the core catcher of the Hole 563 wash core. The core catcher of Core 1 (the first rotary core) contained a white nannofossil-foraminiferal ooze with abundant *Globorotalia mearnsii* (*cultrata*) s.l., common *G. plesiotumida*, *Globoquadrina dehiscens*, *Orbulina universa*, *Sphaeroidinellopsis seminulina*, *S. subdehiscens*, and *Globigerina nepenthes*, which are indicative of foraminiferal Zone N15. Preservation is in general good, but there is a little fragmentation of the foraminiferal tests and some crystalline overgrowth on the globorotaliid forms. The core catchers of Cores 2 and 3 are lower upper Miocene. The composition of the faunas differ from 563-1,CC only in the proportional abundances of the species. *Globigerina nepenthes* is common in these samples, and, because the first appearance datum (FAD) of this species is 12 Ma, the samples are assigned to foraminiferal Zones N15-N14 (10-12 Ma). Fracturing and/or dissolution and overgrowth on many of the globorotaliid fauna are obvious. Sample 563-4,CC is assigned to N14; on the basis of the rare occurrence of *G. nepenthes* it is believed that this sample is close to the upper/middle Miocene boundary and is approximately 12 Ma old. The sample shows considerable dissolution and contains free manganese nodules and manganese infilling of the foraminifers.

#### Miocene (middle)

Sample 563-5,CC at 204 m is either lower N14 or upper N13. This sample contains abundant *Globoquadrina dehiscens*, and common *Sphaeroidinellopsis seminulina*, *S. subdehiscens*, and *Orbulina universa*. It is of particular interest because it contains the tiny spherical calcareous bodies reported from Zone N14 (558-5,CC at 205.5 m). These forms are recognized as *Bolboforma* and described as cysts or reproductive bodies of an unknown Miocene algae. Finding these little bodies in two Leg 82 holes 375 miles apart at the same depth and within the same stratigraphic horizon supports the theory that they may be regional markers in deep-sea sediments. The abundance and preservation of the forami-

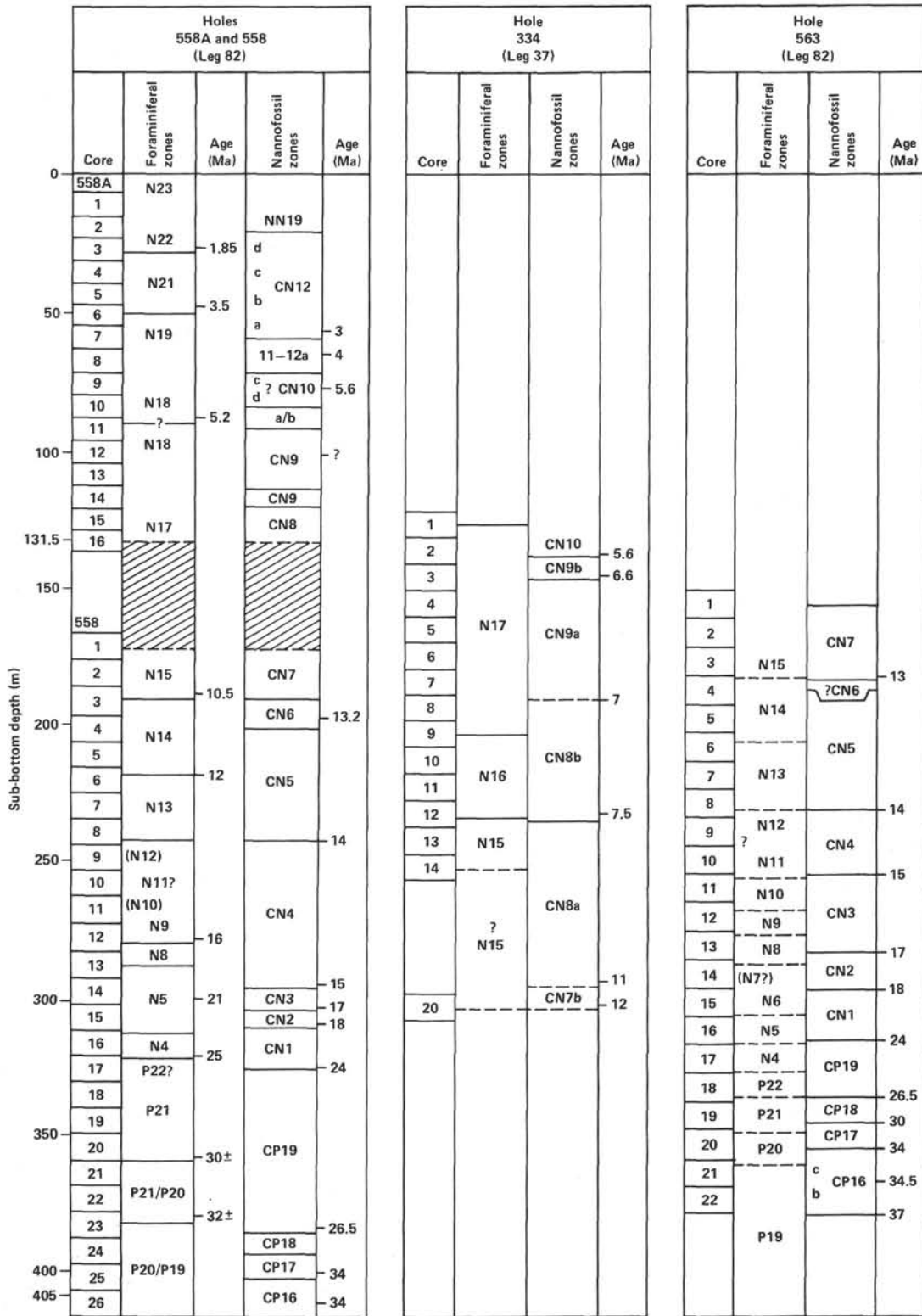


Figure 7. Correlation chart of foraminiferal and nannofossil zones for Holes 558, 558A, 334 (Aumento, Melson, et al., 1977), and 563 (site chapter, Site 563, this volume).

niferal fauna at both sites are similar: in both places there is a marked increase in numbers of *Globoquadrina dehiscens*, and both samples show similar dissolution.

The core catcher of Core 6 is assigned to the lower part of Zone N13 based on the common occurrence of *Globorotalia siakensis* (*mayeri* of some authors) and the associated fauna. The absence of *Globigerina nepenthes* specimens indicates an age older than 12 Ma. Dissolution and fragmentation of the specimens are apparent. Sample 563-7, CC is tentatively assigned to the same zone; in this sample, foraminifers are better preserved and more abundant than the preceding core. It must be pointed out that the zones and ranges assigned in this report are based solely on core catcher samples and that shore-based study of the sections will provide more accurate determinations and better resolution. The core catcher of Core 8 seems to be close to the top of the middle Miocene sequential series of *Globorotalia foehsi*, *G. lobata*, *G. robusta*, *G. foehsi*, *G. peripheroacuta*, and *G. peripheroronda*. In temperate regions large carinate end forms of the *foehsi* lineage are not well developed and that seems to be the case at this site. It is therefore necessary to use other indicators. The *foehsi* lineage and interval zones of the middle Miocene are, in increasing age, N12 (13.2–14.2 Ma), N11 (14.2–15 Ma), N10 (15–15.5 Ma), and N9 (15.5–16 Ma). Lacking the *foehsi* markers to separate these zones, other criteria relied upon indicate that the core catchers of Cores 9 through 11 span these intervals. The core catcher of Core 9 contains abundant *Globorotalia mayeri*, *Sphaerodinellopsis seminulina*, and *S. subdehiscens*; the core catcher of Core 10 has abundant *G. scitula* and other middle Miocene species; and the core catcher of Core 11 has abundant *G. praemenardii*. More precise zonation will be possible after the sections are studied. The core catcher of Core 12 is tentatively assigned to the lower part of N9 or topmost N8. The sample consists of abundant *S. subdehiscens* and *S. seminulina*; common *Globoquadrina dehiscens*, *G. altispira*, *Globorotalia scitula*; and floods of globigerinids in the finest fraction.

#### Miocene (lower)

The core catcher of Core 13 is in the lower Miocene Zone N8, based on the presence of abundant *Globoquadrina dehiscens*, *G. predehiscens*(?), *Catapsydrax dissimilis*, *C. unicus*, and *Sphaerodinellopsis subdehiscens* and the absence of *Orbulina*. The core catchers of Cores 14 and 15 are also lower Miocene and tentatively assigned to N6. The core catchers of Cores 16 and 17 are assigned to N5/N4 based on the assemblage of *G. dehiscens*, *G. venezuelana*, *Catapsydrax dissimilis*, and rare *Globorotalia kugleri*. Rare *G. kugleri* was first observed in 563-16, CC. The last appearance datum (LAD) of this species is approximately 21 Ma old, so this core might be assigned to middle-lower N5, and 563-17, CC may be assigned to Zone N4. Both of these samples have abundant globigerinids.

#### Oligocene

The core catcher of Core 18 is upper Oligocene; the fauna consists of large *Globoquadrina venezuelana*, *G.*

*advena*, *G. tripartita*, *Catapsydrax dissimilis*, and abundant small globigerinids. Tentative assignment is lowermost N4/P22 (24.5–26 Ma) or upper P21 (26 Ma). The core catcher of Core 19 is middle P21. Sample 563-20, CC at 346.5 m contains a large robust group of foraminifers plus abundant *Chiloguembelina* that may be assigned to the lower part of P21 or upper P20. The core catcher of Core 21 seems to be transitional between lower and upper Oligocene. The fauna shows considerable fragmentation, which may be an artifact of the violent reaction with hydrogen peroxide that was noted during washing. Manganese nodules are common. The core catcher of Core 22 is lower Oligocene and assigned to foraminiferal Zone P19 (or to a slightly older zone) based on the presence of *Pseudohastigerina* sp. and the extinction datum of *Globorotalia increbescens*.

#### SEDIMENT ACCUMULATION RATES

Because the upper 156 m of sediment were not recovered, sediment accumulation rates could only be calculated for the upper portion of the lower Oligocene through the middle Miocene. Preliminary age designations show some differences between nannofossil and foraminiferal dates, so we have plotted the age ranges at each core catcher depth and have calculated an average sediment accumulation rate for each stratigraphic interval, based on the boundaries determined from nannofossil and foraminifers respectively (see Fig. 5 and Table 3).

The sediment accumulation rates for the same stratigraphic intervals at Sites 563 and 558, are very similar. In general, the rates are lower in Site 563, which is expected because the sediment section is 42.5 m shorter than at Site 558.

Again, as at Site 558, the most obvious and marked change in sediment accumulation rates occurs near the top of the lower Miocene (from 21.3 to 6.1 m/Ma). This change also corresponds to the lithologic transition between Units 1 and 2.

#### PORE-WATER CHEMISTRY

The results of the interstitial water chemistry analysis for Hole 563 are shown in Figure 8 and tabulated in Table 4.

The values of pH, alkalinity, and chlorinity remain fairly constant with depth. The salinity values, on the other hand, show a sharp increase after crossing the boundary between Lithologic Units 1 and 2 and then decrease with depth. The calcium and magnesium concentration gradients are typical for calcareous pelagic sediments overlying basalt; that is, the pore waters are

Table 3. Sediment accumulation rates, Hole 563.

Stratigraphic unit	Age (Ma)	Nannofossils		Foraminifers	
		Depth (m)	Rate (m/Ma)	Depth (m)	Rate (m/Ma)
middle Miocene	12–16	183–280	24.3	195–280	21.3
lower Miocene	16–24	280–320	5.0	280–320	5.0
upper Oligocene	24–32	320–345	3.1	320–355	4.4
lower Oligocene	32–36	345–365	5.0		

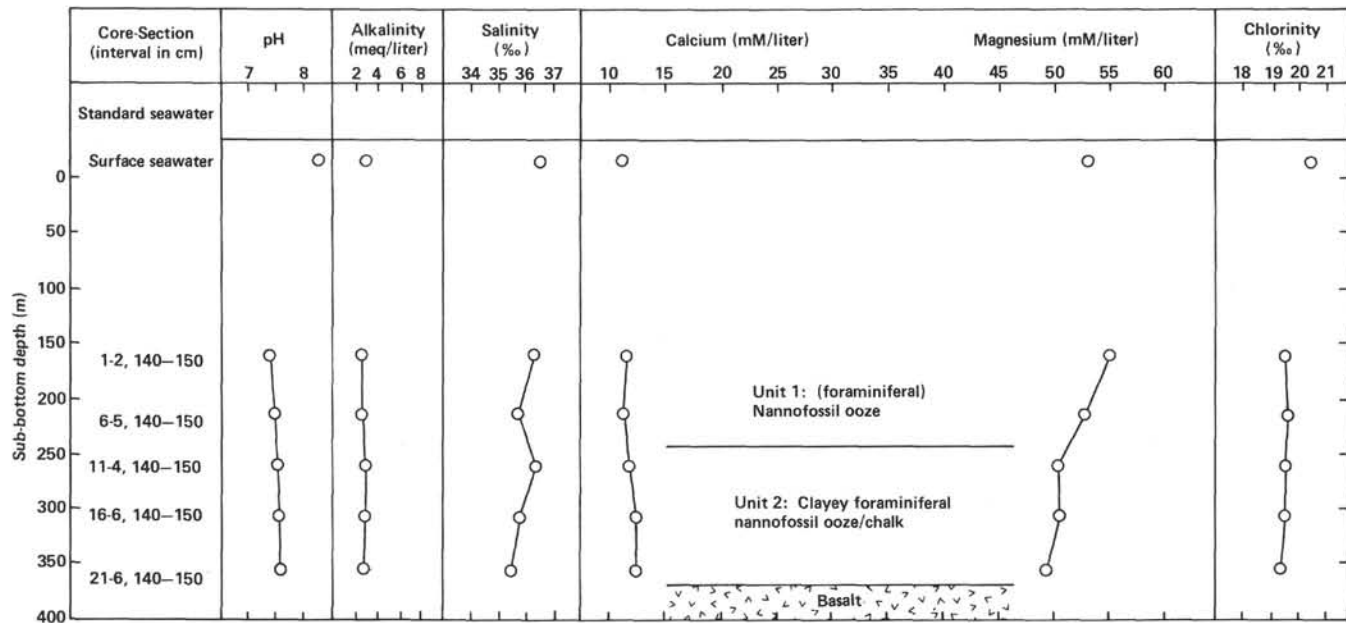


Figure 8. Downhole variations in interstitial water chemistry, Hole 563.

Table 4. Interstitial water chemistry, Hole 563.

Core-Section (interval in cm)	Sub-bottom depth (m)	pH	Alkalinity (meq/liter)	Salinity (‰)	Calcium (mmoles/liter)	Magnesium (mmoles/liter)	Chlorinity (‰)
1-2, 140-150	162	7.43	2.632	36.2	11.59	54.91	19.51
6-5, 140-150	212	7.47	2.541	35.7	11.55	53.29	19.71
11-4, 140-150	260	7.52	2.768	36.4	12.02	50.57	19.61
16-1, 140-150	308	7.48	2.621	35.8	12.51	50.73	19.54
21-6, 140-150	355	7.51	2.402	35.5	12.43	49.39	19.31

enriched in calcium and depleted in magnesium. We note also that rate of change for the concentrations of calcium and magnesium decreases after crossing the boundary between Lithologic Units 1 and 2.

As in Hole 558, we found authigenic dolomite rhombs in the lowermost 10 m of sediment in contact with the basalt, but with much lower concentrations (only 10% by visual estimate as compared to an estimated 30% in Hole 558). However, the calcium and magnesium values did not show anomalous concentrations for the pore-water sample taken in these dolomitic sediments as they did in Hole 558. We can speculate that the abundance of dolomite and the degree of change in the concentration curves of calcium and magnesium are directly related.

**IGNEOUS PETROLOGY AND GEOCHEMISTRY**

Basement rocks were first recovered at 364.5 m sub-bottom depth. We drilled only 18 m into a sequence of homogeneous, fresh to moderately altered pillow basalts, which represent two chemical groups.

**Lithology (Fig. 9)**

The pillows of Site 563 are between 30 and 70 cm thick and are usually rimmed by black glass. Interpillow breccias (hyaloclastites), composed of angular glass clasts ranging in size from a few millimeters to a few centimeters, occur in many places. The clasts are surrounded by

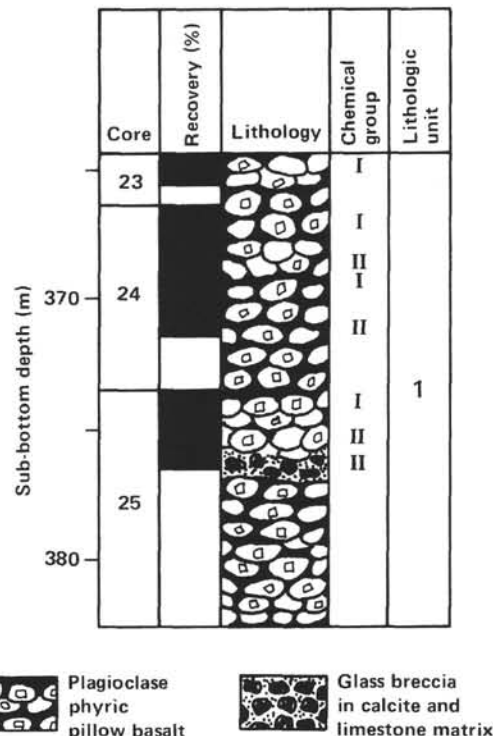


Figure 9. Basement lithology column, Hole 563.

limestone or sparry calcite, which has also filled remaining cavities. Along fractures and at carbonate contacts the glass is altered to thin brown palagonite rinds.

Site 563 basalts are sparsely plagioclase phyric. The plagioclase phenocrysts are randomly scattered (2–3%), most forming elongate to rounded, slightly resorbed glomerocrysts, ranging from 2 to 5 mm in diameter. Minor euhedral to anhedral olivine (less than 2 mm), now completely altered to brown clay, is also present (less than 1%).

Small round vesicles (less than 0.5 mm in diameter) are rare. A few irregular shaped vesicles (less than 7 mm) also occur; these are lined by calcite.

Fractures and veins, filled by either pinkish brown limestone or white sparry calcite, are present throughout the section. In some places vein boundaries are very irregular, with lobe-shaped embayments of limestone into the surrounding basalt.

### Petrography

All pillow basalts examined from Site 563 have the same mineral proportions, with only a variation in grain size and texture of the groundmass. The texture ranges from glomerophyric intergranular to glomerophyric plumose.

Large lath-shaped to prism-shaped plagioclase phenocrysts (0.5–5 mm) with a composition of An<sub>60</sub> (optically determined) make up 5% of the basalt. These glomerophyric phenocrysts are zoned and slightly resorbed, and they contain glass inclusions. Minor amounts of subhedral olivine phenocrysts (0.5–0.8 mm) are partially to fully replaced by brown clay.

The majority of the groundmass consists of equal proportions of randomly oriented, acicular-shaped to lath-shaped plagioclase (40%) and anhedral clinopyroxene (40%), plus 3% equant to granular opaques and 1% granular altered olivine. The last stage of crystallization is represented by either fine-grained intergranular or featherlike arrangements of plagioclase and clinopyroxene. Round to irregular shaped vesicles (0.1–0.8 mm) range from 1 to 10% in volume and usually contain calcite; clay-filled vesicles are rare or absent.

The sample from Core 563-24-2, 123 cm has a hyalophitic plumose texture. It contains only trace amounts

of plagioclase phenocrysts, compared to the other samples.

### Geochemistry

Ten pillow basalts were analyzed from Site 563, forming two chemical groups. Full analyses are presented in Table 5, and results are plotted against sub-bottom depth in Figure 10. Average analyses for the two chemical groups are given in Table 6. Group I and Group II have distinct Fe<sub>2</sub>O<sub>3</sub> contents (10.7 and 9.7%, respectively) and K<sub>2</sub>O contents (0.26 ± 0.06 and 0.12 ± 0.05%, respectively), but otherwise are chemically indistinguishable. These differences in Fe<sub>2</sub>O<sub>3</sub> and K<sub>2</sub>O concentrations between the two groups cannot be easily explained by phenocryst dilution, crystal fractionation, or varying degrees of alteration.

The chemical variation within Group I may, however, be explained by plagioclase addition (Table 7). Dilution of the Group I aphyric sample with 5% plagioclase of composition An<sub>60</sub> (as observed in thin section) yields the average composition of Group I phyric samples (Table 7). The observed CaO concentration is somewhat higher than the calculated concentration, but this could well be due to calcite contamination (see Table 7).

Figure 11 is an extended Coryell-Masuda plot, which illustrates the depleted nature of Site 563 basalts.

## MAGNETICS

### Basalt Paleomagnetism

The very hard basalt and drilling problems forced us to stop coring after 18 m. Twelve oriented minicores were taken for on-board paleomagnetic studies. The intensity of natural remanent magnetization (NRM) ranges from 0.8 to 3.8 × 10<sup>-3</sup> emu/cm<sup>3</sup>, and susceptibility varies from 124 to 200 × 10<sup>-6</sup> emu/cm<sup>3</sup> Oe. The values of NRM and susceptibility for each sample are given in Table 8. Each sample was then subjected to alternating field (AF) demagnetization at various steps until 50% or more of the NRM was randomized. The results are given in Table 8; typical results of AF demagnetization are plotted in Figure 12. The linear decay of orthogonal vectors of magnetization in Figure 12 suggest the presence of univectorial directions of magnetization. Medi-

Table 5. Analyses of major elements (in wt. %) and trace elements (in ppm) of Hole 563 basalts.<sup>a</sup>

Core-Section (interval in cm) (piece number)	Sub-bottom depth (m)	Chemical group	SiO <sub>2</sub>	TiO <sub>2</sub>	Al <sub>2</sub> O <sub>3</sub>	Fe <sub>2</sub> O <sub>3</sub> <sup>b</sup>	MnO	MgO	CaO	K <sub>2</sub> O	P <sub>2</sub> O <sub>5</sub>	Total	Mg'	Ti	V	Sr	Y	Zr	Nb
23-1, 32-35	(2B) 364.8	I	49.87	1.01	15.32	10.48	0.17	7.70	13.46	0.22	0.10	98.33	62	6060	341	86	29.2	58	0.6
24-1, 80-83	(5B) 367.3		49.95	0.99	15.24	10.50	0.15	7.70	13.58	0.22	0.09	98.42	62	5940	332	87	27.9	54	1.9
24-2, 88-91	(3D) 368.9	II	49.95	0.97	15.87	9.56	0.15	7.94	13.58	0.07	0.08	98.17	65	5820	319	84	27.6	55	2.5
24-2, 121-124	(5A) 369.2	I	50.17	1.03	14.43	11.28	0.17	7.88	12.70	0.32	0.09	98.07	61	6180	336	83	29.8	55	2.0
24-4, 38-41	(1C) 371.4		50.08	0.99	15.31	9.77	0.16	8.05	13.27	0.09	0.09	97.81	65	5940	321	86	28.2	52	1.7
25-1, 43-46	(1F) 374.0	II	49.79	0.97	15.77	9.54	0.16	7.75	13.69	0.13	0.09	97.89	65	5820	315	82	27.6	52	1.8
25-2, 39-41	(2A) 375.4		49.66	0.97	15.46	9.53	0.16	7.88	14.28	0.12	0.09	98.15	65	5820	315	85	26.9	60	2.0
25-2, 71-74	(3A) 375.7	I	49.60	0.96	15.54	10.09	0.16	7.52	13.52	0.20	0.08	97.67	63	5760	314	84	27.7	50	0.6
25-2, 79-81	(3B) 375.8		49.68	0.95	15.30	10.96	0.17	7.37	13.38	0.33	0.08	98.22	60	5700	310	84	28.7	54	1.8
25-2, 101-103	(3B) 376.0	II	50.17	0.99	15.49	9.81	0.16	7.68	13.71	0.11	0.11	98.23	64	5940	317	84	27.9	52	1.5

<sup>a</sup> On-board measurements were made on ignited samples. Onshore analyses of loss on ignition are less than 1% in most cases. Compiled data tables at the end of this volume (Appendix) include volatile components.

<sup>b</sup> Total Fe as Fe<sub>2</sub>O<sub>3</sub>.

<sup>c</sup> Mg' is the atomic ratio of 100 × (Mg/[Mg + Fe<sup>2+</sup>]) calculated using an assumed Fe<sub>2</sub>O<sub>3</sub>/FeO ratio of 0.15.

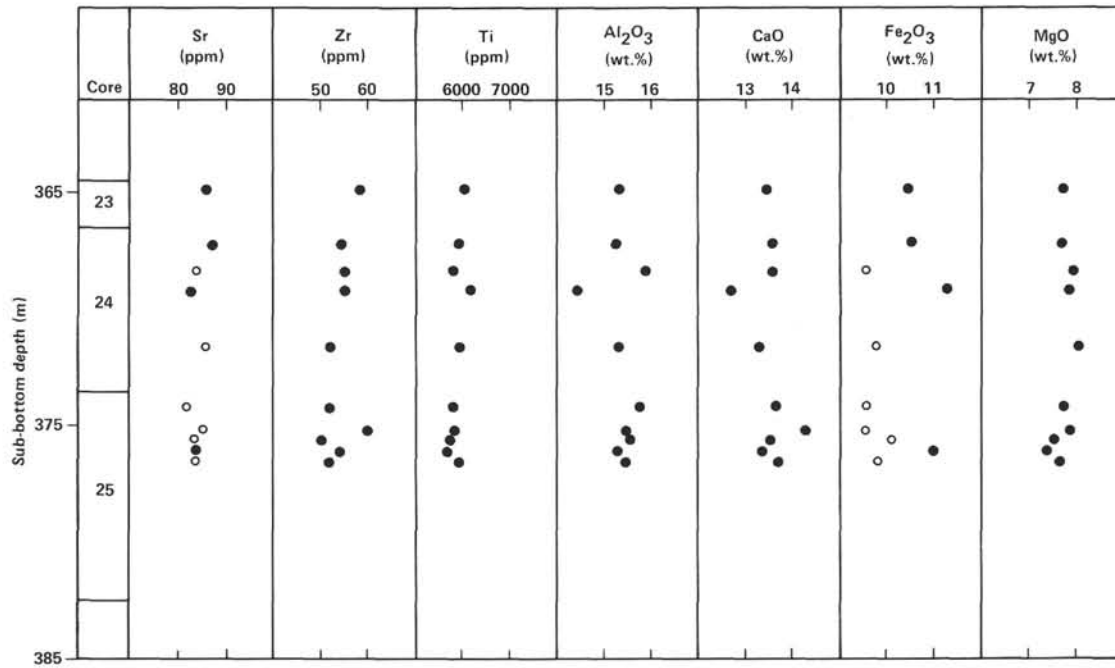


Figure 10. Downhole variations in chemical abundances, Hole 563. In Sr and Fe<sub>2</sub>O<sub>3</sub> columns, closed circles are Chemical Group I and open circles are Chemical Group II.

Table 6. Average analyses of basalt chemical groups from Hole 563.

Element	Aphyric Group I (1) <sup>a</sup>	Phyric Group I (3)		Phyric Group II (6)	
		$\bar{X}$	$\sigma$	$\bar{X}$	$\sigma$
<b>Major element (wt.%)</b>					
SiO <sub>2</sub>	50.17	49.83	0.14	49.90	0.20
TiO <sub>2</sub>	1.03	0.98	0.03	0.98	0.51
Al <sub>2</sub> O <sub>3</sub>	14.43	15.29	0.04	15.60	0.20
Fe <sub>2</sub> O <sub>3</sub>	11.28	10.70	0.30	9.70	0.20
MnO	0.17	0.16	0.01	0.16	0.01
MgO	7.88	7.60	0.20	7.80	0.20
CaO	12.70	13.47	0.10	13.70	0.30
K <sub>2</sub> O	0.32	0.26	0.06	0.12	0.05
P <sub>2</sub> O <sub>5</sub>	0.09	0.09	0.01	0.09	0.01
Mg'	61	62	1	64	1
<b>Trace element (ppm)</b>					
Ti	6180	5900	180	5850	70
V	336	330	20	317	3
Sr	83	86	2	84	1
Y	29.8	28.7	0.7	27.7	0.4
Zr	55	55	1	54	4
Nb	2.0	1.4	0.7	1.7	0.6

Note: Averages are calculated from the data presented in Table 5. Numbers in parentheses are number of samples analyzed.  $\bar{X}$  is median and  $\sigma$  is standard deviation.  
<sup>a</sup> Sample 563-24-2, 121-124 cm.

an demagnetizing field (MDF) for each sample was calculated by plotting the quick plot of NRM percentages at corresponding alternating field used for demagnetization (e.g., Fig. 12). The MDF of most samples is in the range of 150-250 Oe.

The plot of MDF and susceptibility versus depth does not show different units as observed at Site 562. How-

Table 7. Major element modeling of plagioclase dilution in Group I basalts, Hole 563.

Element	Liquid <sup>a</sup>	An <sub>60</sub>	Liquid + 5% An <sub>60</sub>	Observed <sup>b</sup>
SiO <sub>2</sub>	50.17	52.96	50.30	49.83
TiO <sub>2</sub>	1.03	0.98	0.98	0.98
Al <sub>2</sub> O <sub>3</sub>	14.43	29.72	15.16	15.29
Fe <sub>2</sub> O <sub>3</sub>	11.28	0.84	10.78	10.65
MnO	0.17	0.16	0.16	0.16
MgO	7.88	7.50	7.59	7.59
CaO	12.70	12.28	12.68	13.47
K <sub>2</sub> O	0.32	0.13	0.31	0.26
P <sub>2</sub> O <sub>5</sub>	0.09	0.09	0.09	0.09

Note: Concentrations are in wt.%.  
<sup>a</sup> Liquid is the aphyric Group I sample from Table 6.  
<sup>b</sup> Observed composition is the average phyric Group I from Table 6.

ever, based on inclination values (see Fig. 13) two units are recognized as follows. *Unit 1*. This is the upper part of basalt extending from 364.5 to about 375 m; it has positive inclination values. *Unit 2*. This is the lower part of the basalt extending from 375 m to the last cored depth of 377 m; it has negative inclination values.

At this stage, two more samples were collected from Section 563-25-2 to see if the negative inclination values were true or just the result of sample inversion. Then two more samples were taken from core specimens long enough so that there is no doubt of sample inversion. The results from these samples confirmed that the negative inclinations obtained previously from Section 563-25-2 are valid. There is no difference in MDF and susceptibility, so it is most likely that these two units represent two time units rather than two geochemical units. The positive inclinations are in agreement with the location of this site on Magnetic Anomaly 13, whereas nega-

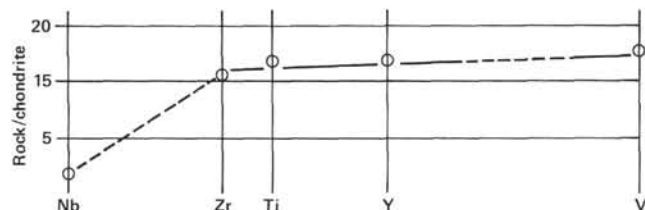


Figure 11. Extended Coryell-Masuda diagram for Hole 563 basalts.

Table 8. Basalt paleomagnetism, Hole 563.

Core-Section (interval in cm)	J <sub>NRM</sub> ( $\times 10^{-3}$ emu/cm <sup>3</sup> )	NRM inc. (°)	Stable inc. (°)	$\chi$ ( $\times 10^{-6}$ emu/cm <sup>3</sup> Oe)	MDF (Oe)
23-1, 104-106	1.70	53.5	52.0	128	210
23-2, 2-4	2.82	45.1	40.8	125	238
24-1, 2-10	3.75	44.9	41.6	190	190
24-1, 74-76	6.21	36.8	45.4	200	195
24-2, 93-95	2.71	41.1	50.5	124	240
24-3, 112-114	2.83	47.7	43.3	133	285
24-4, 28-30	1.50	34.8	33.9	132	315
25-1, 36-38	2.30	51.3	48.4	130	218
25-2, 39-41	1.48	-52.9	-48.1	153	225
25-2, 101-103	0.99	-54.8	-65.1	145	160
25-2, 79-81	0.80	-30.7	-33.3	150	234
25-2, 115-117	1.20	-52.7	-49.7	144	232

Note: J<sub>NRM</sub> = intensity of natural remanent magnetization (NRM); inc. = inclination;  $\chi$  = susceptibility; MDF = median demagnetizing field.

tive inclinations may represent a short reversed subpolarity zone within Anomaly 13.

The fact that the inclination values are (as at most of the earlier Leg 82 holes) shallower than the expected dipole inclination value for the latitude of this site may be explained by tectonic rotation of the crust since the eruption of these basalts.

### Sediment Paleomagnetism-Magnetostratigraphy

Two hundred eight meters of sediments were cored after drilling 156.5 m from the top. The sediment recovered was 85%. As at Hole 558, oriented samples were collected at 25-cm intervals depending on lithology. The lithologic similarity between sediments of this hole and the sediments of Hole 558 suggested that remanence in these samples would be of very low intensity and not measurable on the shipboard Digico spinner magnetometer. After measuring the NRM, we observed that remanent magnetization of samples from Core 563-1 though Section 563-10-4 was below or just above the noise level of the magnetometer. However, as the color of sediments changed from various shades of white in Core 9 to very light brown in Core 10, the remanent magnetization was measurable but still not reliable. However, samples from Section 563-10-5 to Core 18 had remanence measurable on the shipboard magnetometer with reliable results. The samples from Core 18 downhole were again very weakly magnetized and the remanence could not be measured. After measuring NRM, we realized that only 9 of 225 samples had reversed polarity. Two samples were selected for AF demagnetization to check the stability of the directions of magnetization. The results are plotted in Figures 14 and 15. Sample 563-10-5, 9-11 cm shows the presence of an antiparallel component of magnetization (Fig. 14), which is removed at

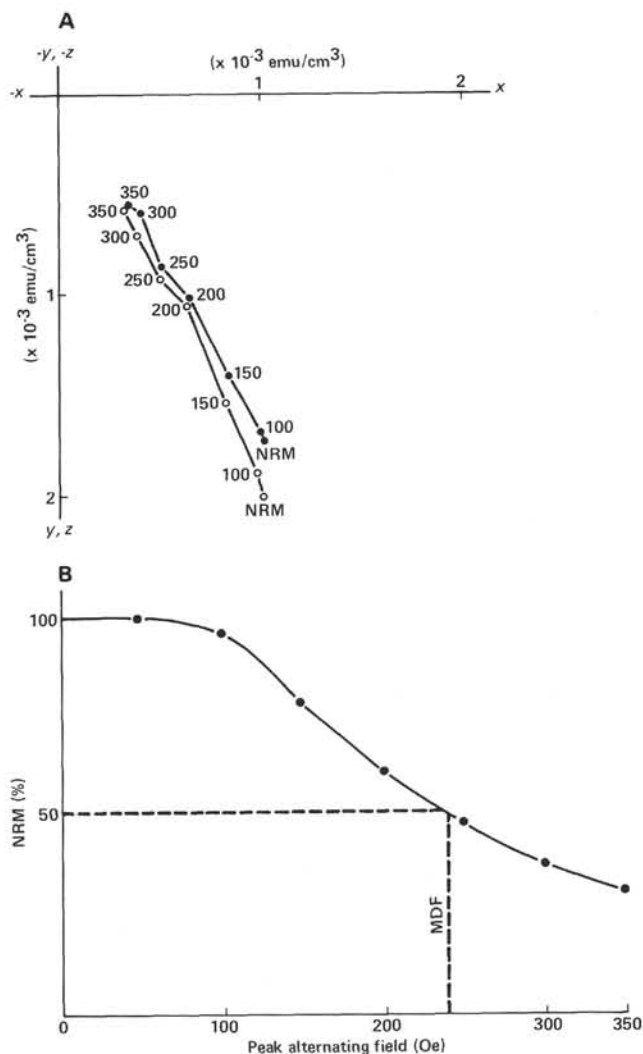


Figure 12. Basalt Sample 563-23-2, 2-4 cm. A. Vector diagram showing the change in NRM after alternating field demagnetization; solid circles are plotted on the horizontal plane and open circles are plotted on the vertical plane. B. Plot of percent natural remanent magnetization (NRM) versus peak alternating field for the determination of the median demagnetizing field (MDF).

75-100 Oe AF demagnetization. MDF of 120 Oe is calculated as shown in Figure 14. The second sample (563-12-2, 91-93 cm) shows a single component of magnetization, and the orthogonal components of magnetization gradually decay to the origin (Fig. 15). This sample has very low MDF (see Fig. 15). These results of AF demagnetization indicate that many of the samples with normal magnetic polarity have a secondary component of magnetization caused by the present magnetic field of the Earth and that this component can be removed by AF demagnetization at 100 Oe. Therefore all samples from Sections 563-10-5 through 563-18-5 were subjected to a single-step AF demagnetization at 100 Oe. The stable inclination values obtained after AF demagnetization are plotted in Figure 16. Negative inclination implies reversed magnetic polarity, and positive inclination means normal magnetic polarity. The sequence of mag-

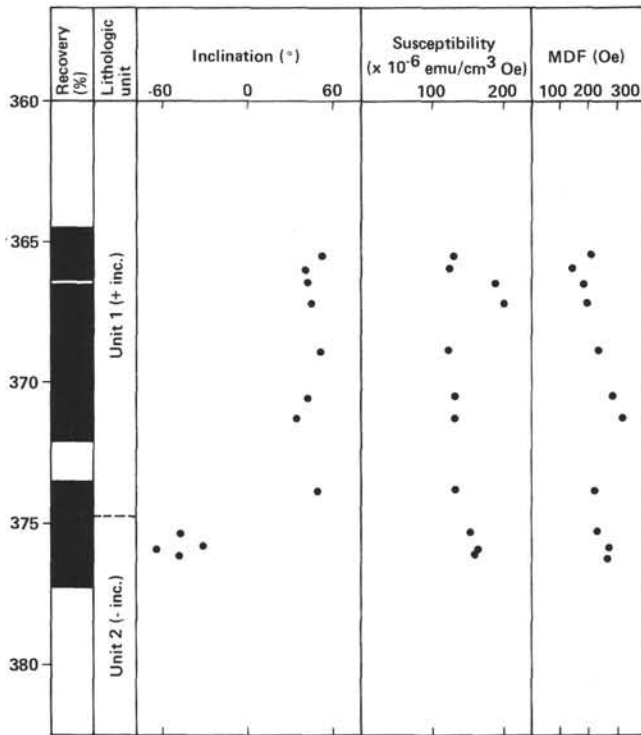


Figure 13. Downhole plot of paleomagnetic properties, Hole 563. MDF = median demagnetizing field.

netic polarity reversals in Figure 16 is based on these data. Single-sample polarity reversals are indicated by an arrow on the left side of the observed polarity sequence.

Using the nannofossil age assignments based on samples from the core catchers and comparing the results of this hole to those of Hole 558, we made the following observations:

1. The Paleogene/Neogene boundary (based on CN zones of Okada and Bukry, 1980) in sediments of Hole 558 occurs between 558-17-3 and 558-19-3, which corresponds to a long zone of reversed magnetic polarity. The same boundary occurs between Cores 563-15 and 563-17 from Hole 563, and there is a long zone of reversed magnetic polarity in Core 563-16. Based on this, the long zone of reversed polarity is correlated with Subchron C6CR (reversed polarity zone between Magnetic Anomalies 6C and 7).

2. Zone CP19 occurs in Core 558-20 and the same core has a long zone of normal magnetic polarity. The Zone CP19 also occurs in Core 563-18, and there is a long zone of normal polarity in 563-18 and the lower part of 563-17. This implies that the two long normal polarity zones can be correlated to each other. Knowing that the magnetostratigraphy is more elaborate for Hole 558 and having correlated this polarity zone with Subchron C8N (Magnetic Anomaly 8), we also correlated the long normal polarity zone in Core 563-18 and the lower part of 563-17 to the Subchron C8N.

The long normal polarity zone in Core 558-16 is correlated to magnetostratigraphic Chron 19 and the core catcher sample from the same core shows Zone CN2. The same Zone CN2 is recorded in the core catcher sam-

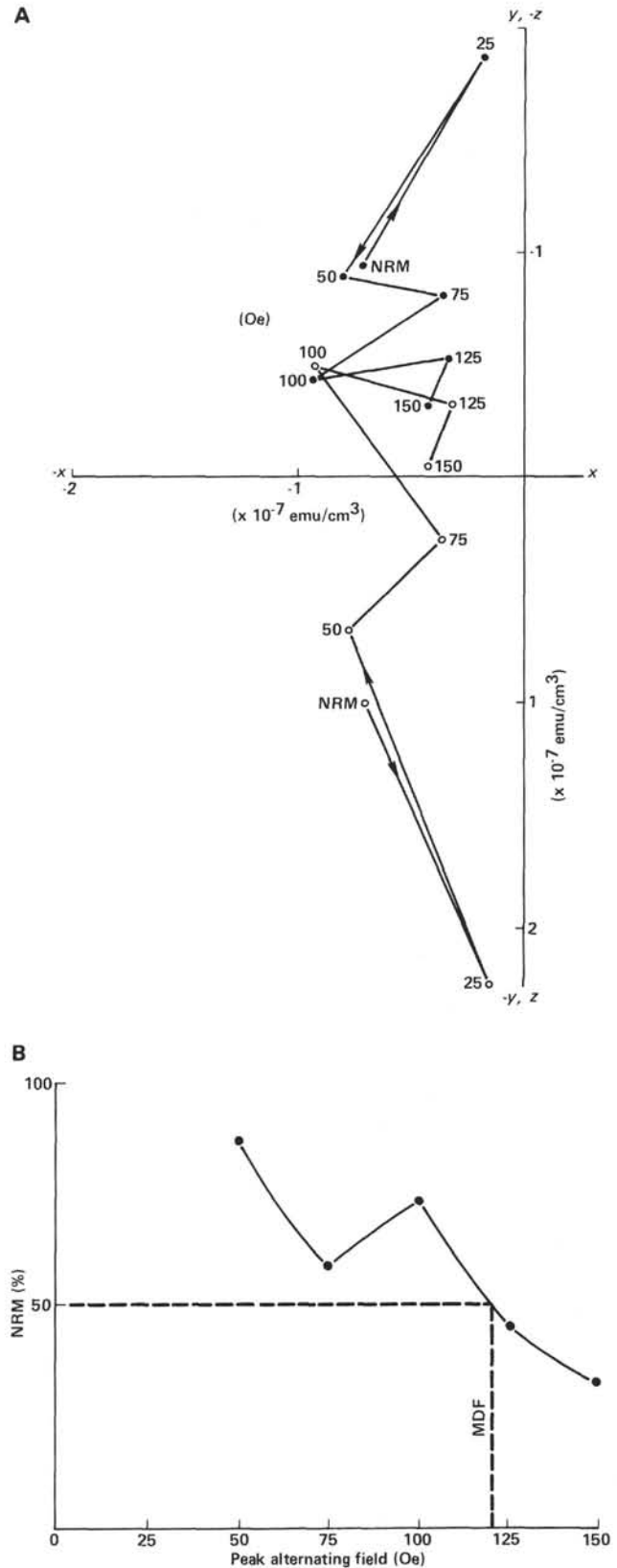


Figure 14. Sedimentary Sample 563-10-5, 9-11 cm. A. Vector diagram showing the change in NRM after alternating field demagnetization; solid circles are plotted on the horizontal plane and open circles are plotted on the vertical plane. B. Plot of percent natural remanent magnetization (NRM) versus peak alternating field for the determination of the median demagnetizing field (MDF).

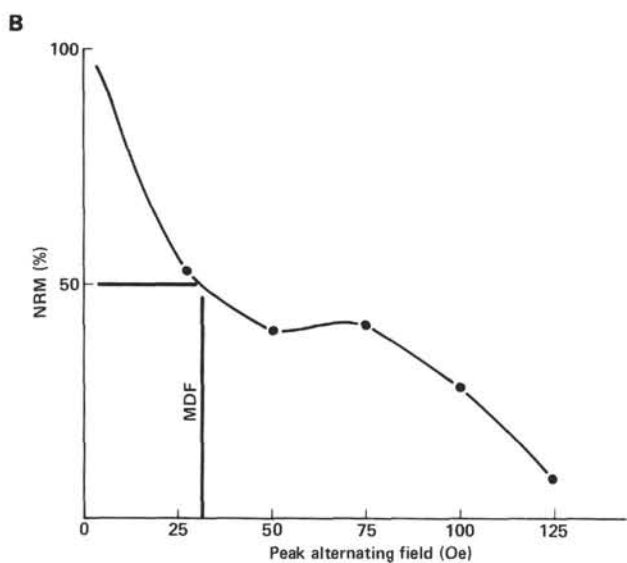
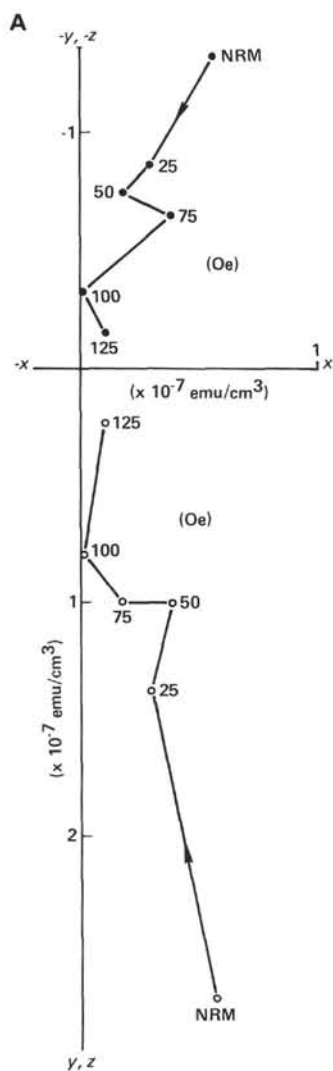


Figure 15. Sedimentary Sample 563-12-2, 91-93 cm. A. Vector diagram showing the change in NRM after alternating field demagnetization; solid circles are plotted on the horizontal plane and open circles are plotted on the vertical plane. B. Plot of percent natural remanent magnetization (NRM) versus peak alternating field for the determination of the median demagnetizing field (MDF).

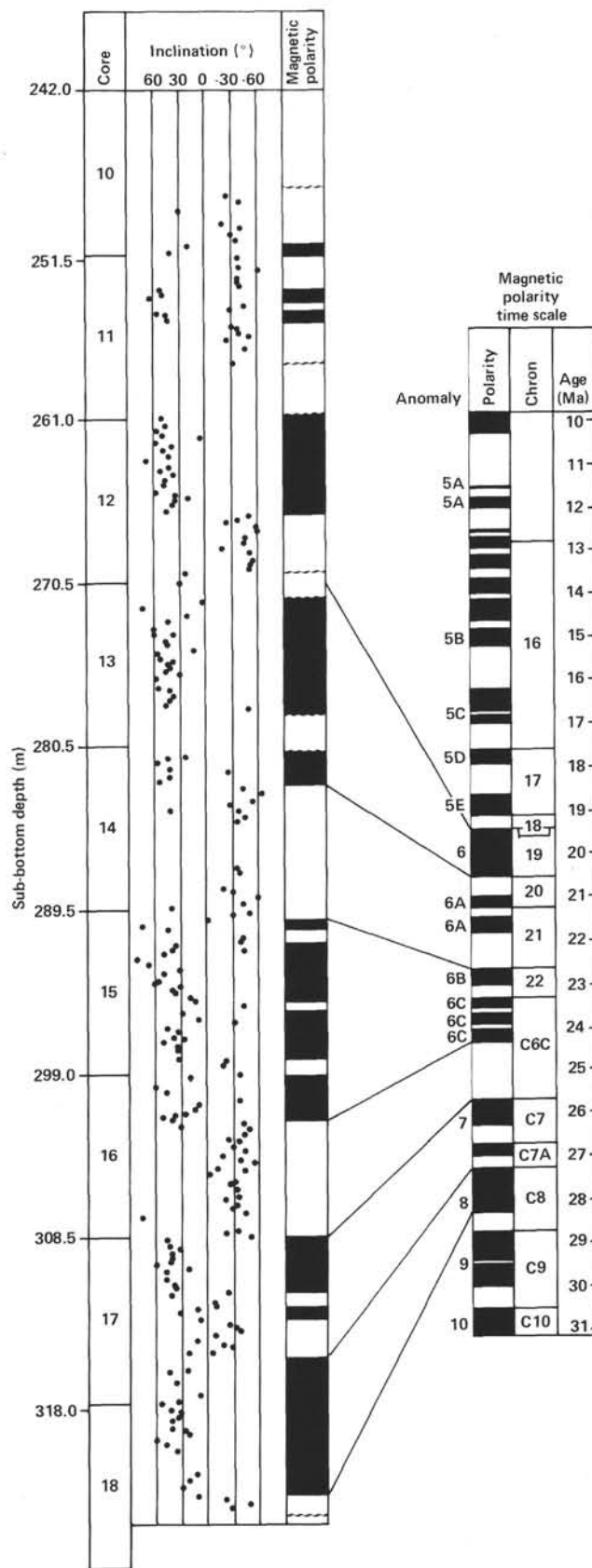


Figure 16. Correlation chart of magnetic inclinations and polarities with the magnetic polarity time scale of Lowrie and Alvarez (1981) for Hole 563.

ple from Core 563-14, but there is no long normal polarity zone. However, there is a long normal polarity zone in Core 563-13. If this is correlated to Chron 19, it implies a higher sedimentation rate for sediments of this age in Hole 563. This is also suggested by the preliminary work done (see Sedimentology and Biostratigraphy section), which shows Zone CN3 in Cores 11 through 13. Keeping this in mind, we correlated the long normal polarity zone of Core 563-13 to the magnetostratigraphic Chron 19.

On the basis of the evidence discussed here, the observed magnetic polarity reversal sequence is tentatively correlated to the standard magnetic polarity time scale, as shown in Figure 16. For a complete discussion of magnetostratigraphic results see Khan et al., this volume.

### PHYSICAL PROPERTIES

It was intended that this site would be continuously cored and a full suite of logs run and would thus provide a second opportunity (after Site 558) to compare the physical property values obtained by laboratory and downhole measurements. Because of the premature operation of the bit-release mechanism after only a very shallow penetration of basement, the hole was abandoned without logging. A systematic pattern of measurements of density, porosity, seismic velocity, and thermal conductivity was made and will be discussed below in separate sections for sediment and basalt basement data. All measured physical property values are shown in Table 9.

#### Sedimentary Section

The sediments consisted of a sequence of calcareous oozes showing progressive compaction down the hole. The effect of the disturbance of rotary coring on these soft sediments was extensive, as is described in the Sedimentology and Biostratigraphy section. Determining useful physical property values from such cores is made difficult not only by the drilling disturbance, but also by the problem of sampling soft core material.

Density was measured by the continuous GRAPE technique on all core sections. Although the data from this method are affected by the degree of drilling disturbance, they should detect density variations in a qualitative manner. Comparison to downhole density logs should allow estimation of the error in continuous GRAPE data caused by drilling effects. Such a study will await shore-based processing of the GRAPE data.

For discrete sampling, the cylinder technique was used. Despite the difficulty of obtaining the sample without deformation, this is probably the best technique available. Two-minute GRAPE measurements were made on all samples; and gravimetric density, porosity, and grain density measurements will be made onshore. Additional samples were taken for shipboard bulk-density determination by cutting cubes of firm sediment and wrapping them in plastic film. This was unsuccessful because of the friability of the sediment.

Seismic velocities were measured on the working half of core sections while they were still in their liners. De-

spite the inherent inaccuracy of this method, the plotted data (Fig. 17) show a low degree of scatter. There is a suggestion of a cyclical pattern of changes in velocity in the central part of the section that may correspond to cyclical variation in sediment lithology. The wavelength of these cycles is 10 to 15 m. No clear correlation with the lithology has been established.

Thermal conductivity was measured once per core by the needle-probe technique on core sections that had been allowed to equilibrate to laboratory temperature for several hours. The data are plotted against sub-bottom depth in Figure 18, with the data for Site 558 for comparison. The measurements have not been corrected to *in situ* values; this correction would produce a lowering of all values by less than 5%. The error in determined values is estimated at less than 10%. The rotary-cored sections of Holes 558 and 563 produce a scatter of points in Figure 18 that form one population and indicate increasing conductivity with depth. This is a feature explained by increasing compaction. Points determined from the piston-cored section of Hole 558A also show increasing conductivity with depth, but with a nonlinear trend that is not continuous with that found for the rotary-cored sequences. The discontinuity in the values may be a product of the increased disturbance of rotary cores, which has the effect of destroying some of the *in situ* compaction effect.

On Figure 18 is shown the mean trend of thermal conductivity values with depth determined by Hyndman and others (1974) for carbonate sediments in the Indian Ocean. Values found in this study are markedly higher than Hyndman's, but the cause of this difference has not yet been established.

Shear-strength measurements were made on the first few cores recovered, but because of the great variability caused by deformation of the cores, the testing was discontinued. The Torvane instrument was used for all measurements.

The variation of physical properties shown in Figure 17 correlates with the lithology. The transitional boundary between Lithologic Units 1 and 2 occurs over the depth range from 230 to 270 m; this is reflected in an increase in density and thermal conductivity, although there is no clear increase in seismic velocity. The velocity increases steadily down the core with a possible cyclic trend visible over the depth range 270 to 320 m. This may well be due to the alternation of lithification between ooze and chalk within the upper part of Unit 2.

#### Basement Section

The two cores recovered from basement contained dominantly basalt rock, which was sampled for velocity and density measurements. Velocity was measured on minicore samples for horizontal velocity and on slices from the working half core for vertical velocity. The same samples were used for 2-minute GRAPE measurements; then the minicore was used as a paleomagnetic sample, and the rock slice was used for bulk density determination. Values of velocity and density show no trend within the small depth range sampled and are within a typical range for ocean basalts.

Table 9. Physical properties measurements for Hole 563.

Core-section (interval in cm)	Sub-bottom depth (m)	Sonic velocity (km/s)		T (°C)	Thermal conductivity (mcal/(cm-deg-s))	GRAPE density (g/cm <sup>3</sup> )		Gravimetric density			Vane shear strength (g/cm <sup>2</sup> )	Lithology or remarks
		V.	H.			V.	H.	Wet-bulk density (g/cm <sup>3</sup> )	Water content (%)	φ (%)		
1-1, 27-31	158.8	1.60		22		1.78		1.65	32	53	2300	Pale ooze mod. deformed
1-1, 137-139	157.9	1.62		22							2000	Mod. deformed
1-2, 7-9	158.1	1.66		22								Very deformed
1-2, 96-98	159.0	1.63		22	3.53							Very deformed
2-2, 21-23	167.7	1.66		22							2300	Mod. deformed
2-2, 139-141	168.9	1.58		22							1000	
2-4, 10-12	170.6	1.59		22					33			Very deformed
2-4, 126-128	171.8	1.60		22	3.49							
3-2, 12-14	177.1	1.59		22							1200	
3-2, 135-137	178.4	1.59		22		1.87					1100	Cylinder sample
3-4, 8-10	180.9	1.60		22					34		1200	
3-4, 127-129	181.3	1.59		22	3.73						1200	
4-2, 9-11	186.6	1.60		22							1700	Moderately-very deformed
4-2, 110-112	187.6	1.59		22	3.59						1500	
5-2, 10-12	196.1	1.58		22							1300	Very deformed
5-2, 143-145	197.4	1.60		22							1500	
5-4, 10-12	199.1	1.60		22		1.82			33			Cylinder sample
5-4, 127-129	200.3	1.58		22	3.55							
5-6, 10-12	202.1	1.59		22								
5-6, 140-142	203.4	1.61		22								
6-2, 15-17	205.6	1.61		22								
6-2, 133-135	206.8	1.61		22	3.57							Moderately disturbed
6-4, 140-142	209.9	1.62		22					32			
6-6, 135-137	212.8	1.64		22								
7-2, 122-124	216.2	1.59		22								
7-4, 10-12	218.1	1.60		22					33			
7-4, 127-129	219.3	1.61		22	3.82	1.91						
7-6, 132-134	222.3	1.63		22								
8-2, 68-70	225.2	1.61		22								
8-4, 6-9	227.6	1.60		22	3.80				33			Cylinder sample
8-4, 126-128	228.8	1.62		22								
8-6, 138-140	231.9	1.67		22								
9-2, 123-125	235.2	1.64		22								
9-3, 65-68	236.2	1.66		22		1.82		1.54	32	49		Bulk density
9-4, 48-50	237.5	1.62		22	3.75	1.85			31			Cylinder sample
9-4, 115-123	238.2	1.64		22								
9-6, 16-18	240.2	1.62		22								
9-6, 118-120	241.2	1.66		22								
9-7, 35-37	241.9	1.65		22								
10-2, 100-102	244.5	1.65		22								
10-4, 19-21	246.7	1.65		22					32			Brown coloration
10-4, 129-131	247.8	1.65		22	3.64							
10-4, 145-147	248.0	1.69		22		1.83		1.02	34	56		Bulk density
10-6, 12-14	249.6	1.69		22								Light yellowish brown
10-6, 137-139	250.9	1.69		22								Pale brown
11-1, 11-13	251.6	1.65		22								Pale brown
11-1, 141-143	252.9	1.65		22								
11-2, 18-20	253.2	1.67		22								
11-2, 127-129	254.3	1.62		22								Color darkens
11-4, 29-31	256.3	1.66		22					31			
11-4, 125-127	257.3	1.68		22	4.43	1.91						Cylinder sample
12-2, 104-106	263.6	1.64		22								
12-4, 65-67	266.2	1.66		22					29			
12-4, 101-105	266.5	1.66		22		1.82		1.67	27	45		Bulk density
12-4, 127-129	266.8	1.63		22	4.00							
12-6, 133-135	269.8	1.70		22								
13-2, 133-135	273.3	1.64		22								
13-4, 99-101	276.0	1.67		22	4.10							
13-5, 106-110	277.5	1.69		22		1.93						Cylinder sample
13-5, 120-122	277.7	1.69		22								
14-2, 37-39	281.9	1.66		22								Core 14 very deformed
14-3, 131-133	284.3	1.65		22								
15-2, 21-23	291.2	1.66		22								
15-4, 16-18	294.2	1.64		22					31			
15-4, 117-119	295.2	1.66		22	3.97							Cylinder sample
15-5, 136-139	296.9	1.66		22		1.90						
15-6, 132-134	298.3	1.67		22								
16-2, 122-124	301.7	1.69		22								
16-4, 122-124	304.7	1.66		22	3.92				28			
16-6, 43-45	306.9	1.63		22								
17-2, 125-127	311.3	1.65		22								
17-4, 15-17	313.2	1.70		22					29			Core 17 very disturbed
17-4, 129-131	314.3	1.66		22	4.08							
18-2, 114-116	320.7	1.66		22								
18-4, 37-39	322.9	1.64		22								
18-4, 129-131	323.8	1.70		22	3.92							
19-2, 15-17	329.2	1.65		22		1.88						Cylinder sample
19-2, 114-116	330.2	1.65		22	4.10				28			
20-2, 18-20	338.7	1.65		22								
20-5, 111-113	344.1	1.67		22					29			
21-2, 144-146	349.5	1.69		22								
21-3, 73-75	350.2	1.69		22		1.95						Cylinder sample
21-4, 23-25	351.2	1.69		22								
21-4, 121-126	352.2	1.67		22	4.40							
21-6, 124-126	355.3	1.69		22								
22-2, 65-67	357.7	1.73		22								
22-2, 98-100	358.0	1.73		22		1.92		1.68	28	46		Bulk density
22-2, 126-130	358.3	1.75		22	4.71							
22-3, 135-137	359.9	1.70		22								
23-1, 105-107	365.6	5.71		22		2.87		2.86	3	7		
23-1, 116-122	365.7		5.56	22			2.84					
24-1, 8-10	366.6	5.42		22		2.78						
24-1, 86-90	367.4		5.57	22			2.86	2.84	3	8		
24-3, 136-138	370.9	5.43		22		2.79						
24-3, 140-144	370.9			22				2.87	2	6		

Note: V. = vertical, H. = horizontal; water content is corrected; φ = porosity. All values measured at laboratory temperature and pressure. For details of techniques, see Explanatory Notes chapter (this volume).

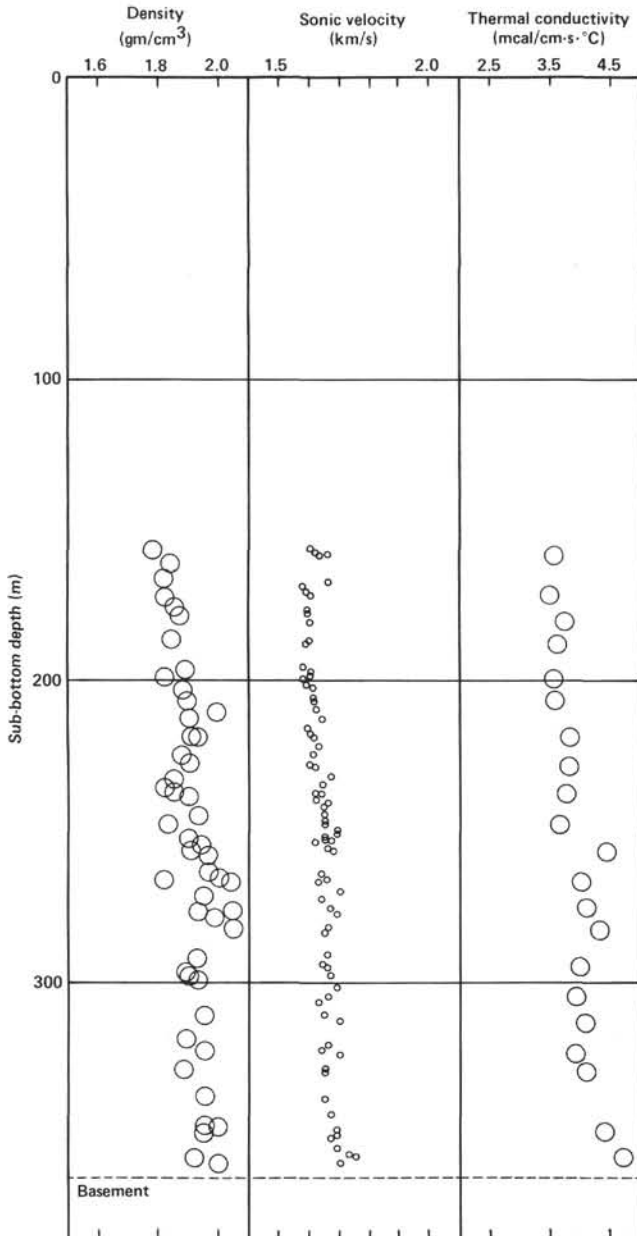


Figure 17. Physical property variations in the sediment section of Hole 563. Size of symbols is proportional to the measured errors.

**SUMMARY AND CONCLUSIONS**

Hole 563 was drilled on Anomaly 13 on the same flow line as Hole 562. The lower part (156.5–364 m) of the sediment column, which was continuously cored, showed the same major change in the rate of sedimentation near the lower/middle Miocene boundary as was observed at Site 558. From here, the correlation can be extended to Sites 556 and 558, which are also on Anomaly 13. This change in sediment accumulation rate oc-

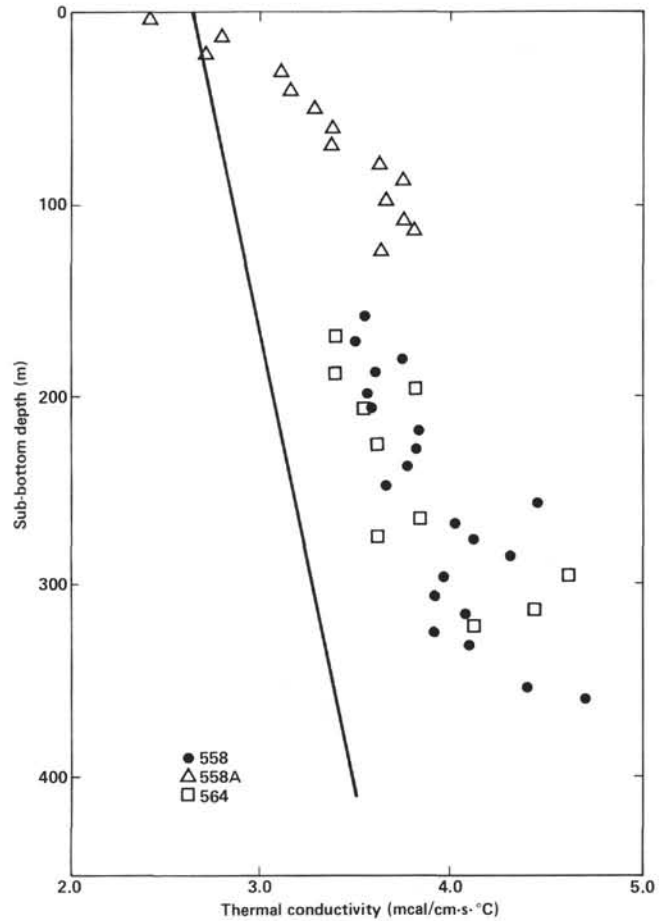


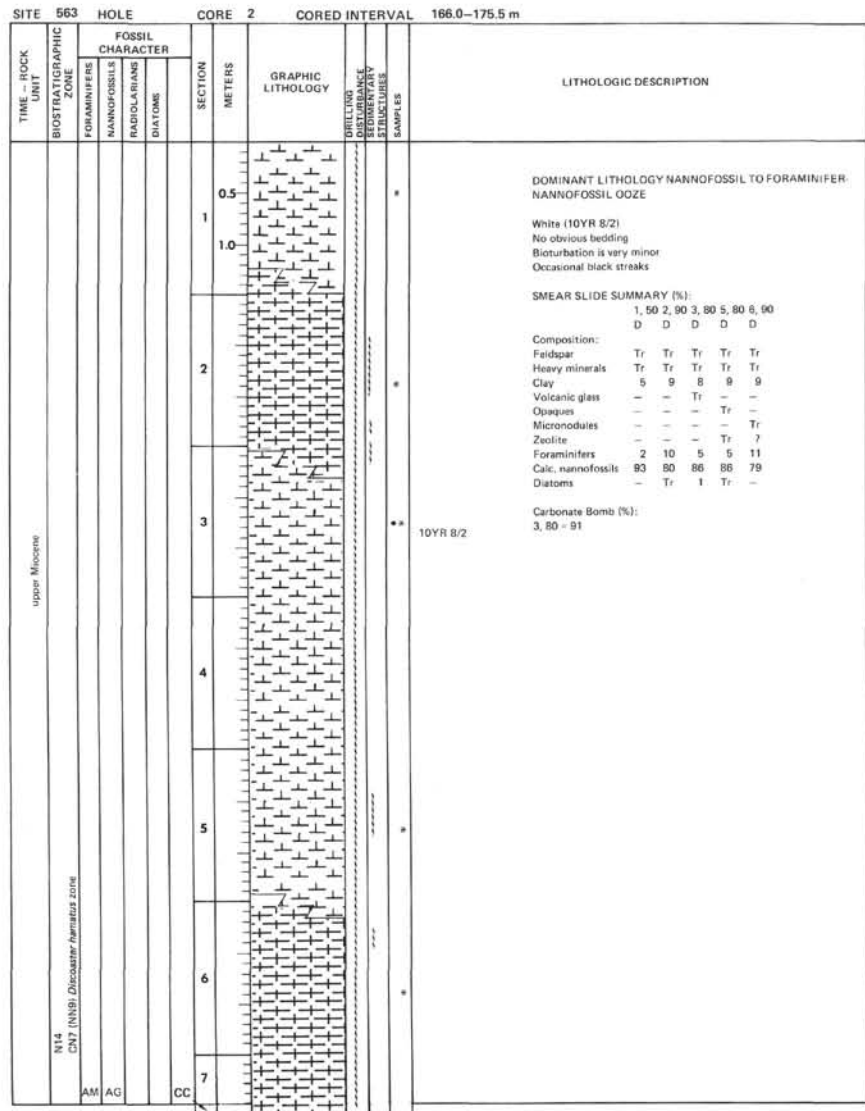
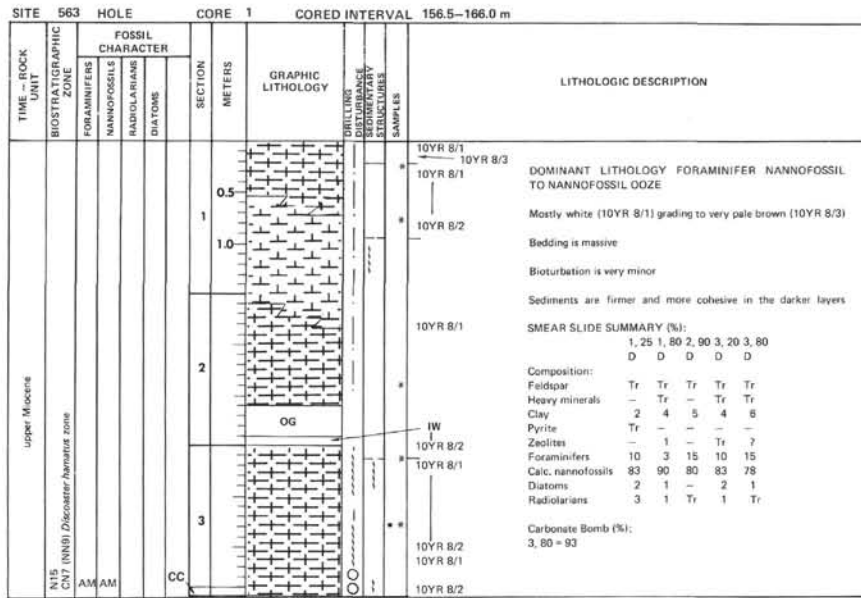
Figure 18. Thermal conductivity plotted against sub-bottom depth for Holes 558, 558A, and 564. Line represents Indian Ocean data from Hyndman et al., 1974. The equation for the line is  $2.65 + 0.002d$ , where  $d$  is sub-bottom depth.

curing near to the time of the early/middle Miocene boundary can then be considered as a general event in this part of the Atlantic.

The basement was only cored for 18.5 m because of difficult drilling conditions and premature bit release. The basement consists of one petrographic unit of sparsely plagioclase phyric basalts, in which two chemical groups are identified. The magmaphile element results indicate a depleted character,  $(Nb/Zr)_{ch} = 0.3$ .

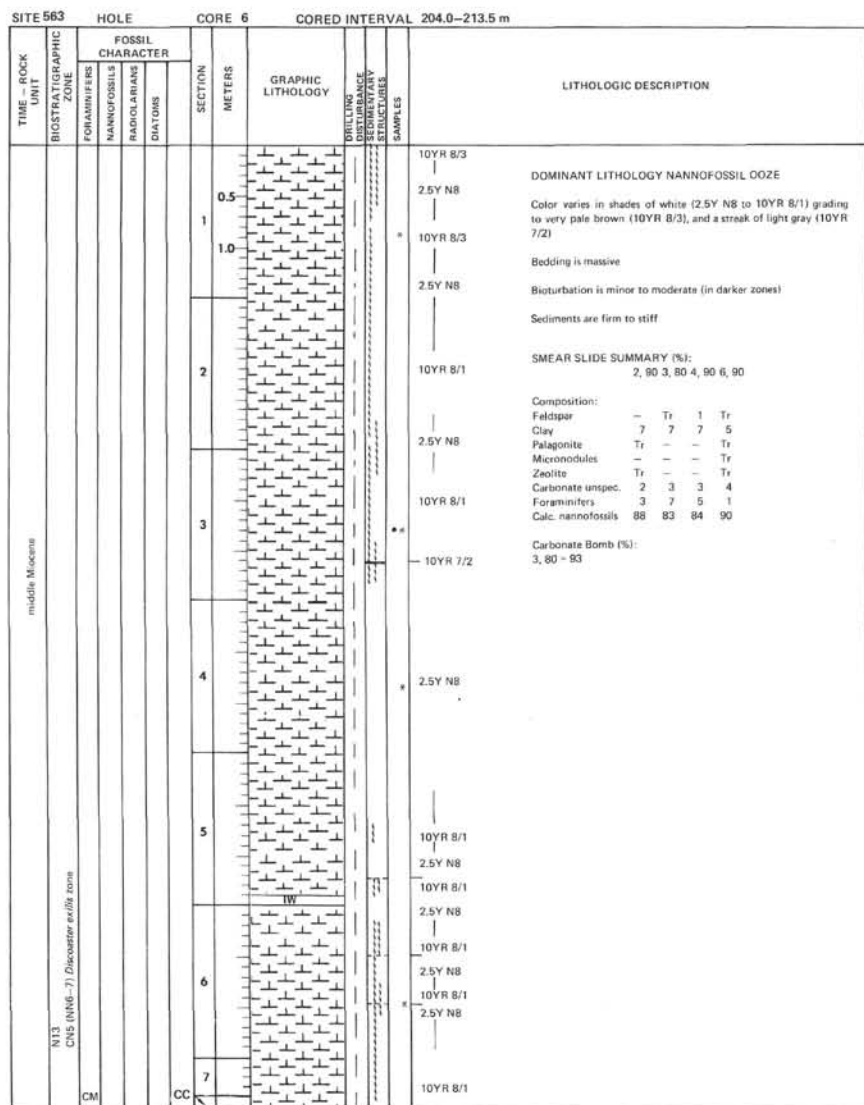
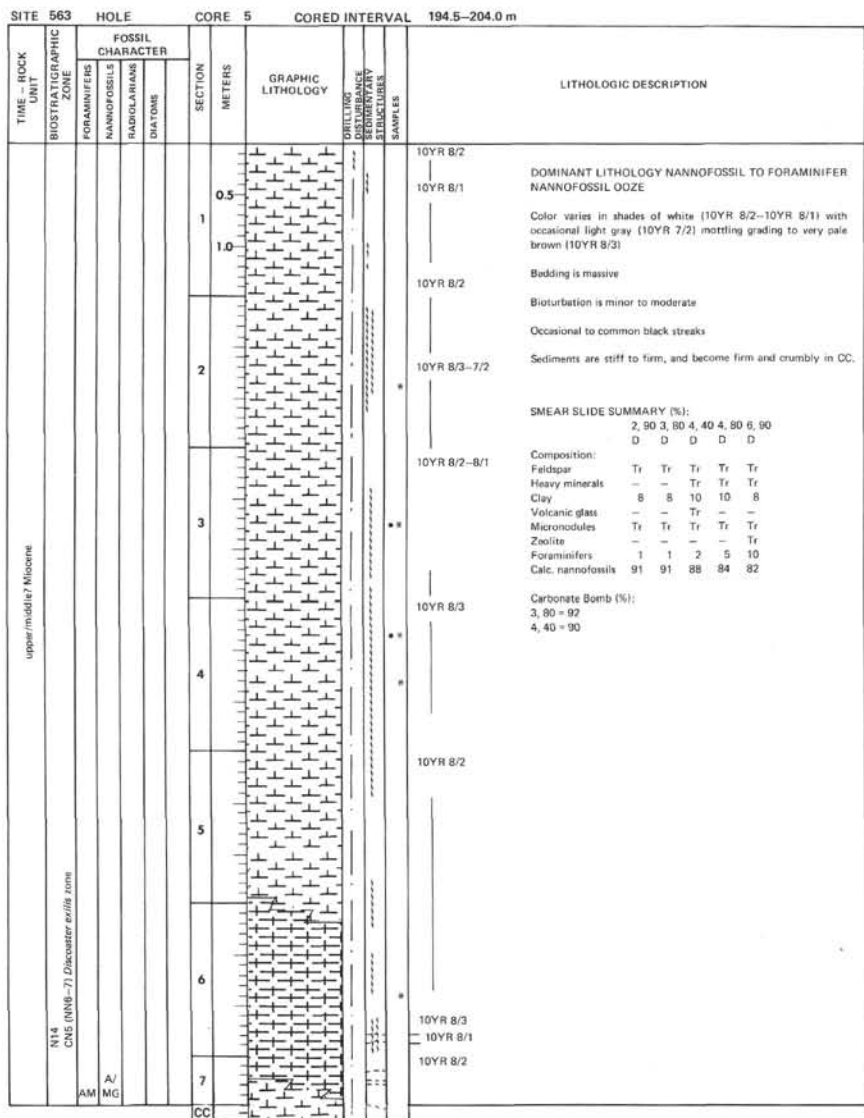
**REFERENCES**

Aumento, F., Melson, W. G., et al., 1977. *Init. Repts. DSDP*, 37: Washington (U.S. Govt. Printing Office).  
 Hyndman, R. D., Erickson, A. J., and Von Herzen, R. P., 1974. Geothermal measurements on DSDP Leg 26. *In* Davies, T. A., Luyendyk, B. P., et al., *Init. Repts. DSDP*, 26: Washington (U.S. Govt. Printing Office), 451–464.  
 Lowrie, W., and Alvarez, W., 1981. One hundred million years of geomagnetic polarity history. *Geology*, 9:392–397.  
 Okada, H. and Bukry, D., 1980. Supplementary modification and introduction of code numbers to the low latitude coccolith biostratigraphic zonation. *Mar. Micropaleontol.*, 5(3):321–325.



SITE 563		HOLE		CORE 3		CORED INTERVAL 175.5-180.0 m		
TIME - ROCK UNIT	BIOSTRATIGRAPHIC ZONE	FOSSIL CHARACTER			SECTION METERS	GRAPHIC LITHOLOGY	LITHOLOGIC DESCRIPTION	
		FORAMINIFERS	NANNOFOSSILS	RADIOLARIANS				DIATOMS
Upper? Miocene	N14 CN7 (INN8) <i>Discosaster hamatous</i> zone	AM	AG				10YR 7/1 10YR 8/2	
		0.5						DOMINANT LITHOLOGY FORAMINIFER-NANNOFOSSIL TO NANNOFOSSIL OOZE  Dominant color is very pale brown (10YR 7/3) which grades from light gray (10YR 7/1) in Section 1 and grades to light brownish gray (10YR 6/2) in Section 6.  Bedding is massive  Bioturbation is minor  Occasional black streaks  SMEAR SLIDE SUMMARY (%): 1, 50 2, 90 3, 80 5, 80 6, 90 D D D D D  Composition: Feldspar Tr Tr Tr Tr Tr Heavy minerals Tr Tr ? - - Clay 9 9 7 7 8 Volcanic glass Tr Tr - - - Palagonite - - - Tr - Micronodules 1 - 1 - Tr Zeolite Tr Tr Tr - - Carbonate unspec. - - - 1 1 Foraminifers 5 8 10 15 12 Calc. nannofossils 84 82 83 77 79 Diatoms - Tr - - Tr  Carbonate Bomb (%): 3, 80 = 93
		1.0						
		2						10YR 7/3
		3						10YR 7/3
		4						10YR 7/3 10YR 6/2 10YR 7/3 10YR 7/3
5						10YR 7/3		
6						10YR 7/3 10YR 6/2 10YR 7/3 10YR 7/3		
CC						10YR 7/3		

SITE 563		HOLE		CORE 4		CORED INTERVAL 185.0-194.5 m		
TIME - ROCK UNIT	BIOSTRATIGRAPHIC ZONE	FOSSIL CHARACTER			SECTION METERS	GRAPHIC LITHOLOGY	LITHOLOGIC DESCRIPTION	
		FORAMINIFERS	NANNOFOSSILS	RADIOLARIANS				DIATOMS
upper/middle? Miocene	N14 CN8 (INN8-7) <i>Discosaster exilis</i> zone	AM	MG				10YR 7/3	
		0.5						DDMINANT LITHOLOGY CLAYEY NANNOFOSSIL, NANNOFOSSIL TO FORAMINIFER NANNOFOSSIL OOZE  Dominant color alternates in shades of white (10YR 8/2-10YR 8/1) which grade from very pale brown (10YR 7/3) in Section 1 and to pinkish white (7.5YR 8/2) in Sections 3 and 4.  Bedding is massive  Bioturbation is minor to moderate  Occasional black streaks  Sediments are generally stiff  SMEAR SLIDE SUMMARY (%): 1, 80 2, 90 3, 54 3, 129 D D D D  Composition: Mica - - Tr - - Clay 15 11 9 8 Palagonite Tr Tr Tr Tr Micronodules 1 Tr 1 Tr Zeolite Tr Tr - - Carbonate unspec. 2 1 2 - Foraminifers 8 7 13 5 Calc. nannofossils 74 80 74 85 Fish remains - - 20 Dolomite - - Tr -  Carbonate Bomb (%): 3, 54 = 89
		1.0						
		2						10YR 8/2 void 10YR 8/3 10YR 7/2 10YR 8/2
		3						void 7.5YR 8/2 10YR 8/2 7.5YR 8/2 10YR 8/2 10YR 8/1
		CC						void

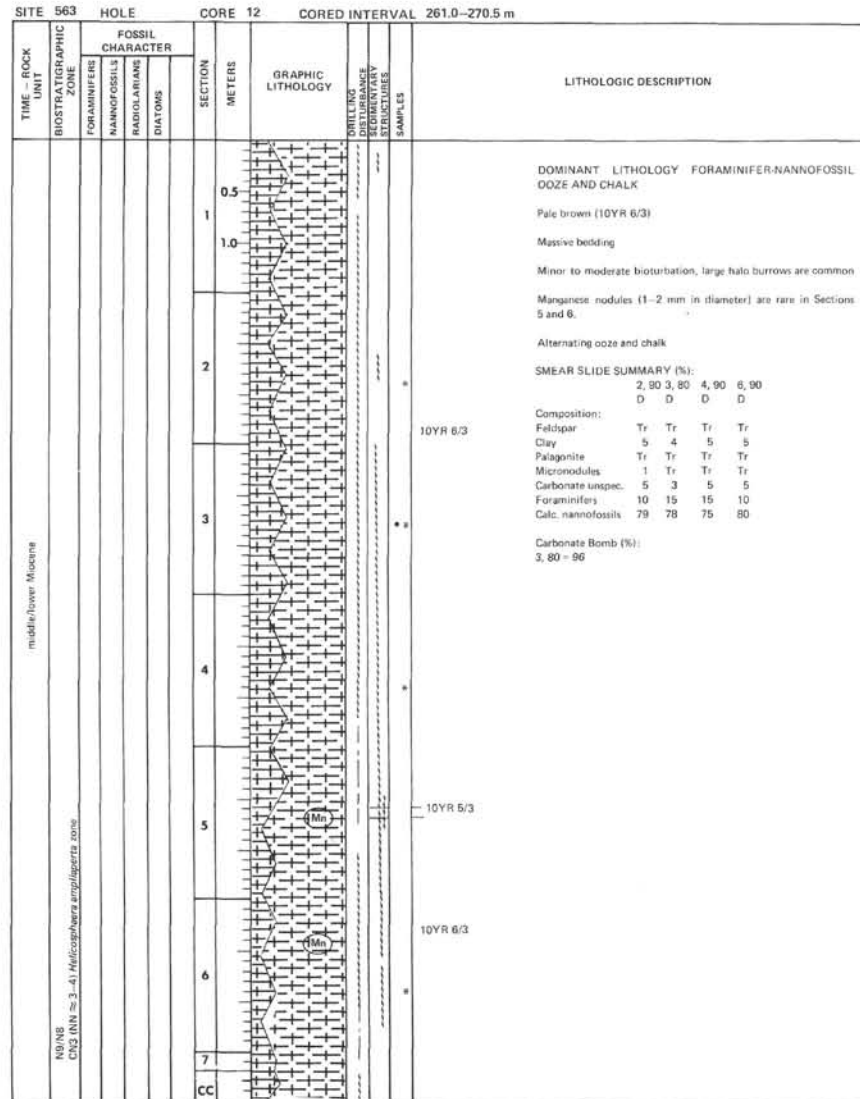
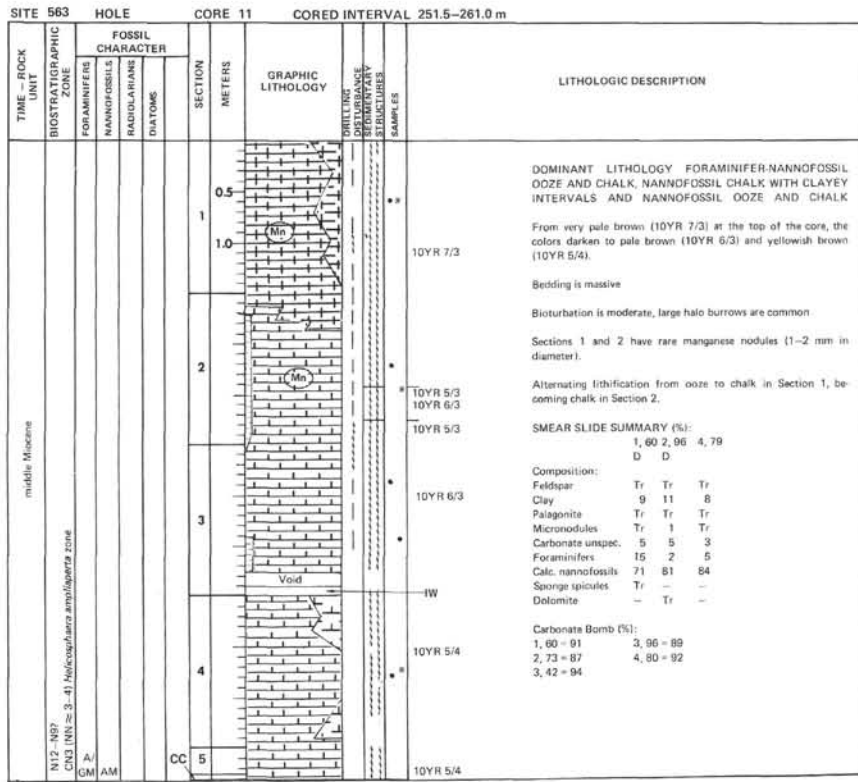


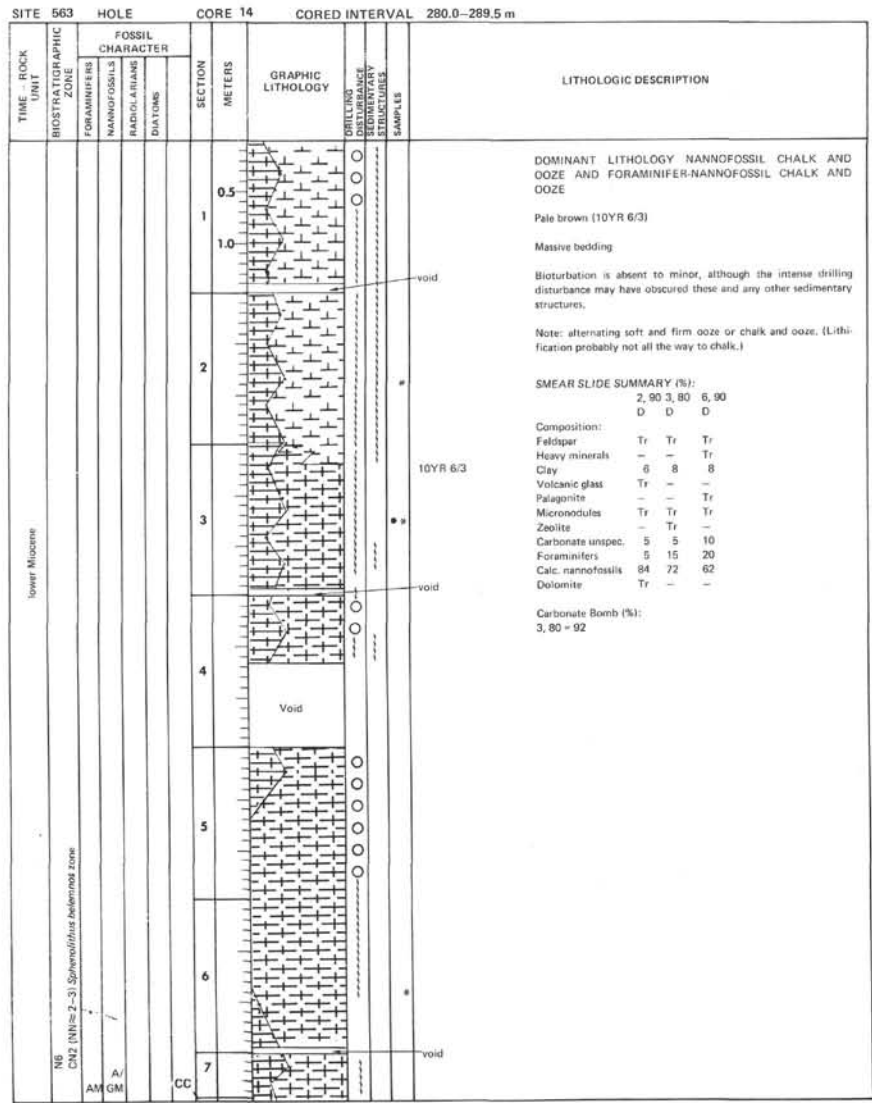
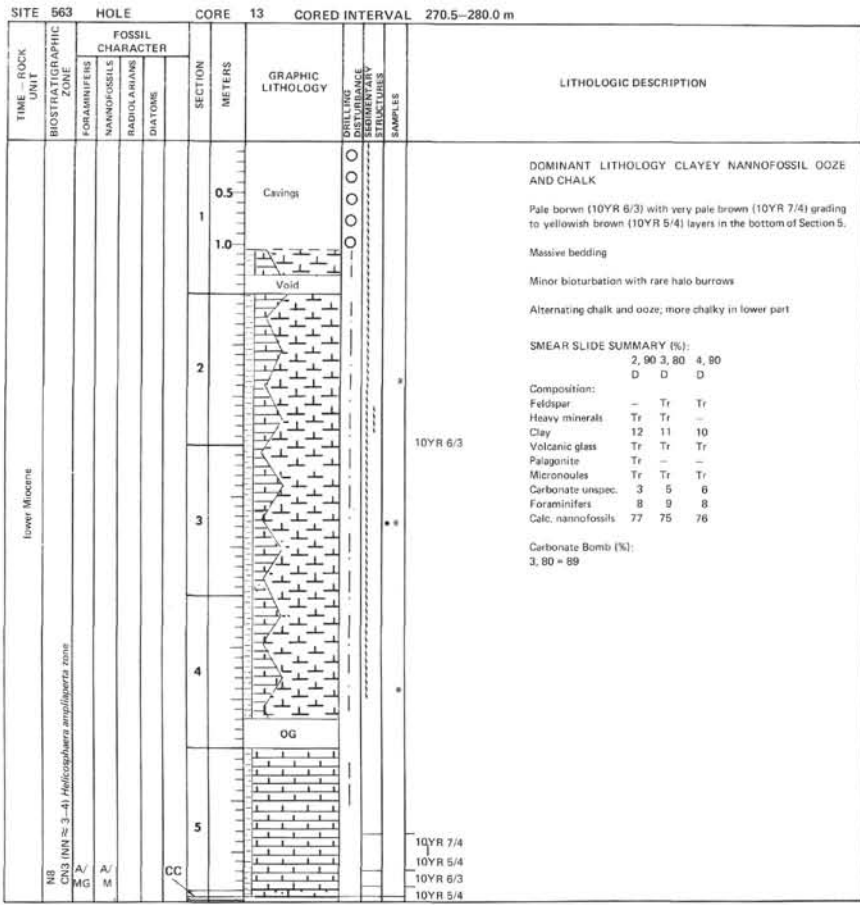
SITE 563		HOLE		CORE 7		CORED INTERVAL 213.5-223.0 m	
TIME - ROCK UNIT	BIOSTRATIGRAPHIC ZONE	FOSSIL CHARACTER			SECTION METERS	GRAPHIC LITHOLOGY	LITHOLOGIC DESCRIPTION
		FORAMINIFERS	NANNOFOSSILS	RADIOLARIANS			
middle Miocene	N13P CNS (NNG-7) <i>Discoaster exilis</i> zone	A/ AG	A/ AG		0.5		<p>DOMINANT LITHOLOGY NANNOFOSSIL OOZE</p> <p>White (10YR 8/1-2.5Y NB)</p> <p>Bedding is massive</p> <p>Bioturbation varies from absent to moderate</p> <p>Core is badly disturbed by drilling</p> <p>SMEAR SLIDE SUMMARY (%):</p> <p>3, 80 5, 90</p> <p>D D</p> <p>Composition:</p> <p>Feldspar Tr Tr</p> <p>Clay 6 9</p> <p>Micronodules Tr 1</p> <p>Zeolite Tr -</p> <p>Carbonate unspec. - 5</p> <p>Foraminifera 5 7</p> <p>Calc. nannofossils 89 78</p> <p>Carbonate Bomb (%):</p> <p>3, 80 - 94</p>
					1.0		
					2		
					3		
					4		
					5		
					6		
7							
CC							

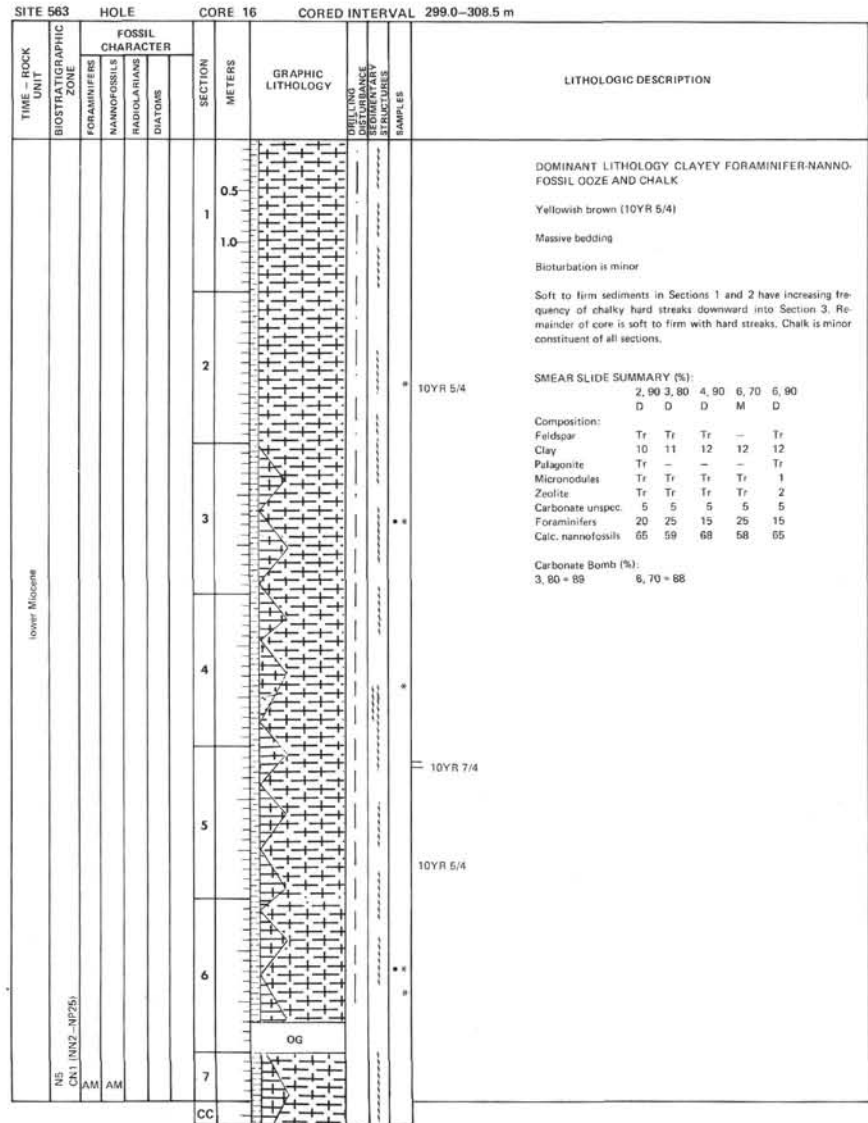
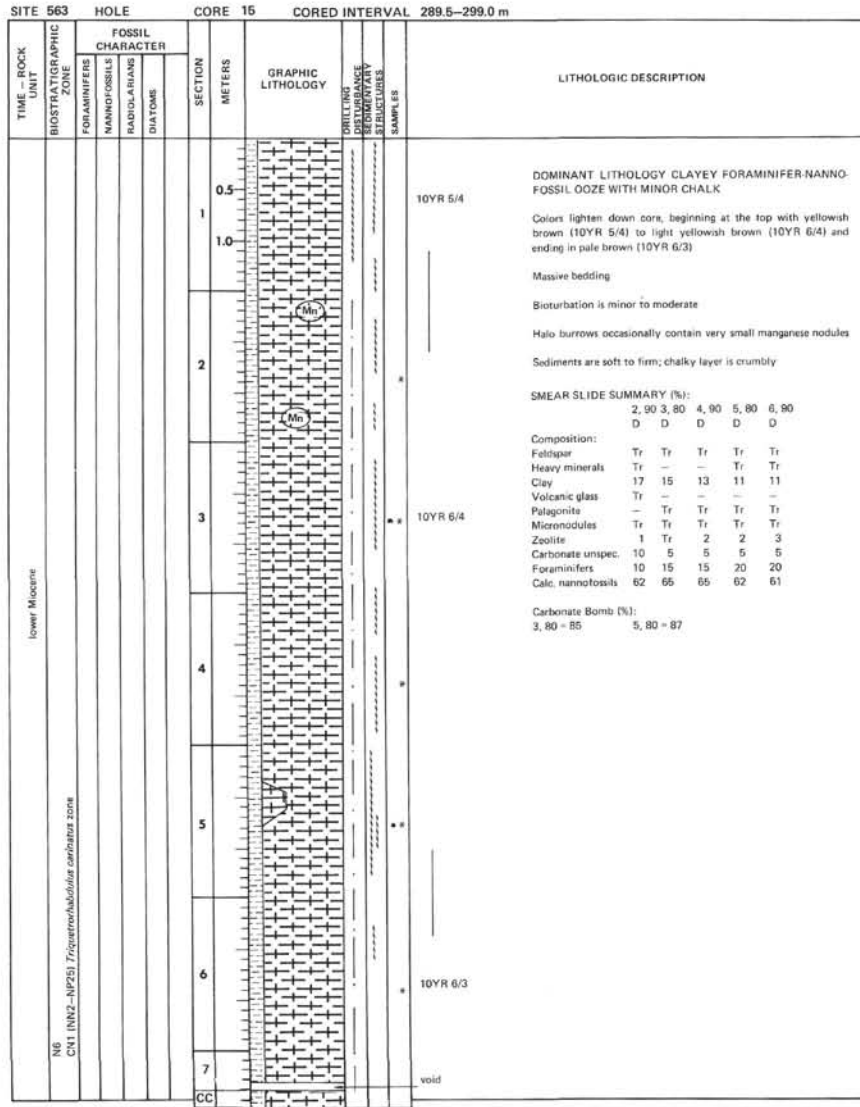
SITE 563		HOLE		CORE 8		CORED INTERVAL 223.0-232.5 m	
TIME - ROCK UNIT	BIOSTRATIGRAPHIC ZONE	FOSSIL CHARACTER			SECTION METERS	GRAPHIC LITHOLOGY	LITHOLOGIC DESCRIPTION
		FORAMINIFERS	NANNOFOSSILS	RADIOLARIANS			
middle Miocene	N13/N12 CNS (NNG-7) <i>Discoaster exilis</i> zone	A/ AG	A/ AG		0.5		<p>DOMINANT LITHOLOGY NANNOFOSSIL OOZE</p> <p>White (10YR 8/1-2.5Y NB)</p> <p>Bedding is massive</p> <p>Bioturbation varies from absent to very minor</p> <p>Core is badly disturbed by drilling</p> <p>SMEAR SLIDE SUMMARY (%):</p> <p>2, 90 3, 80 4, 90 6, 90</p> <p>D D D D</p> <p>Composition:</p> <p>Feldspar - Tr Tr Tr</p> <p>Clay 8 7 7 7</p> <p>Palagonite - - - Tr</p> <p>Micronodules Tr Tr Tr Tr</p> <p>Carbonate unspec. 3 2 3 3</p> <p>Foraminifera 8 8 9 3</p> <p>Calc. nannofossils 81 83 81 87</p> <p>Carbonate Bomb (%):</p> <p>3, 80 - 93</p>
					1.0		
					2		
					3		
					4		
					5		
					6		
7							

SITE 563		HOLE		CORE 9		CORED INTERVAL 232.5-242.0 m	
TIME - ROCK UNIT	BIOSTRATIGRAPHIC ZONE	FOSSIL CHARACTER			SECTION METERS	GRAPHIC LITHOLOGY	LITHOLOGIC DESCRIPTION
		FORAMINIFERS	NANNOFOSSILS	RADIOLARIANS			
middle Miocene	N12-NB CN4 (INN = 1) <i>Sphenofusus heteromorphus</i> zone	AM	AM				
					0.5	10YR 8/1	DOMINANT LITHOLOGY FORAMINIFER-NANNOFOSSIL OOZE TO CLAYEY FORAMINIFER-NANNOFOSSIL OOZE in Section 4, 35-55 cm and Section 5, 140 cm to the bottom of the cored interval.
					1.0	10YR 8/2 10YR 8/1	
					2	10YR 8/2	Colors alternate in shades of white (10YR 8/1-10YR 8/2). In the portions of the core with slightly higher clay content colors gradually darken to very pale brown (10YR 8/3), light gray (10YR 7/1) and pale brown (10YR 8/3). Except for the last meter the core is very deformed from drilling. Darker zones less deformed. Bioturbation is minor to intense. In Section 7 the first occurrence of halo burrows is noted. Bedding is massive.
					3	10YR 8/2	SMEAR SLIDE SUMMARY (%): 2, 80 4, 80 6, 110 7, 40 D D D D M Composition: Feldspar Tr 1 Tr Tr Clay 9 7 11 11 Palagonite - Tr Tr Tr Micronodules 1 Tr Tr Tr Zeolites Tr - - Tr Carbonate unspec. 2 3 5 6 Foraminifers 10 19 13 5 Calc. nannofossils 77 70 71 78 Fish remains - - Tr - Dolomite Tr - -
					4	10YR 8/3	Carbonate Bomb (%): 1, 80 = 94 5, 80 = 90 2, 80 = 89 6, 50 = 87 3, 80 = 97 6, 110 = 89 4, 42 = 86 7, 36 = 90 4, 80 = 92
					5	10YR 8/1-8/2	
			6	10YR 7/4			
			7	10YR 8/3 10YR 7/1 10YR 8/1 10YR 8/3			
			CC				

SITE 563		HOLE		CORE 10		CORED INTERVAL 242.0-251.5 m	
TIME - ROCK UNIT	BIOSTRATIGRAPHIC ZONE	FOSSIL CHARACTER			SECTION METERS	GRAPHIC LITHOLOGY	LITHOLOGIC DESCRIPTION
		FORAMINIFERS	NANNOFOSSILS	RADIOLARIANS			
middle Miocene	N12-NB CN4 (INN = 5) <i>Sphenofusus heteromorphus</i> zone	A/	MG				
					0.5	10YR 7/3	DOMINANT LITHOLOGY FORAMINIFER-NANNOFOSSIL OOZE AND CHALK WITH CLAYEY FORAMINIFER-NANNOFOSSIL OOZE at Section 5, 105-120 cm.
					1.0	10YR 7/3	
					2	10YR 7/3	Very pale brown (10YR 7/3) to brown (10YR 5/3) at clayey interval Bedding is massive Bioturbation is moderate, large halo burrows are common Rare manganese nodules throughout core (2-4 mm in diameter) Lithification alternates between chalk and ooze; Section 6 is all chalk
					3	10YR 7/3	SMEAR SLIDE SUMMARY (%): 3, 80 5, 102 5, 105 6, 90 D D D D Composition: Feldspar Tr Tr Tr Tr Heavy minerals Tr - - - Clay 5 9 14 7 Palagonite - Tr - - Micronodules Tr - Tr Tr Zeolite - Tr - - Carbonate unspec. 5 5 5 5 Foraminifers 20 25 15 20 Calc. nannofossils 70 61 66 68 Dolomite Tr - - Tr
					4	10YR 7/3	Carbonate Bomb (%): 1, 85 = 93 5, 104 = 91 2, 80 = 92 5, 106 = 86 3, 80 = 95 6, 80 = 93 4, 80 = 91
					5	10YR 5/3	
			6	10YR 7/3			
			7				
			CC				







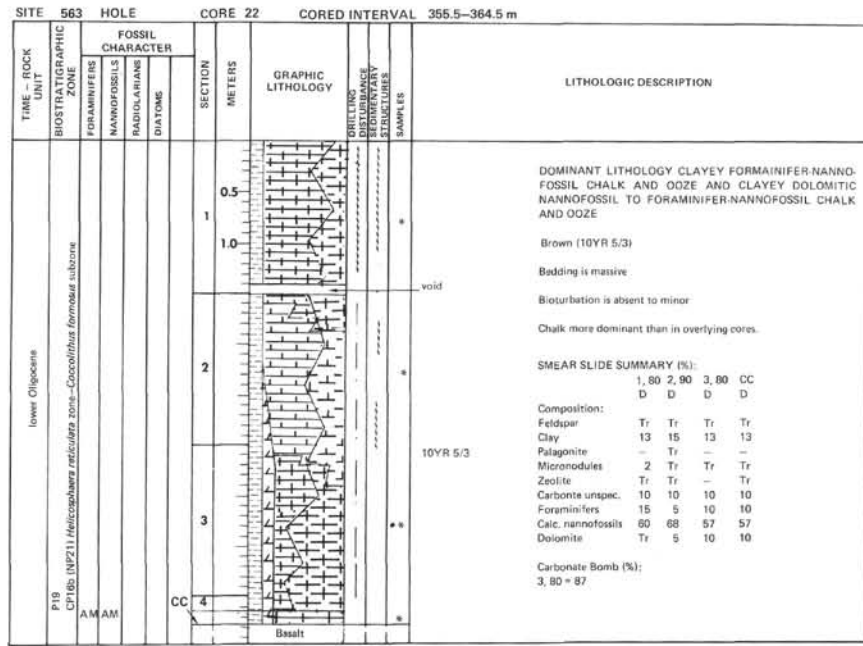
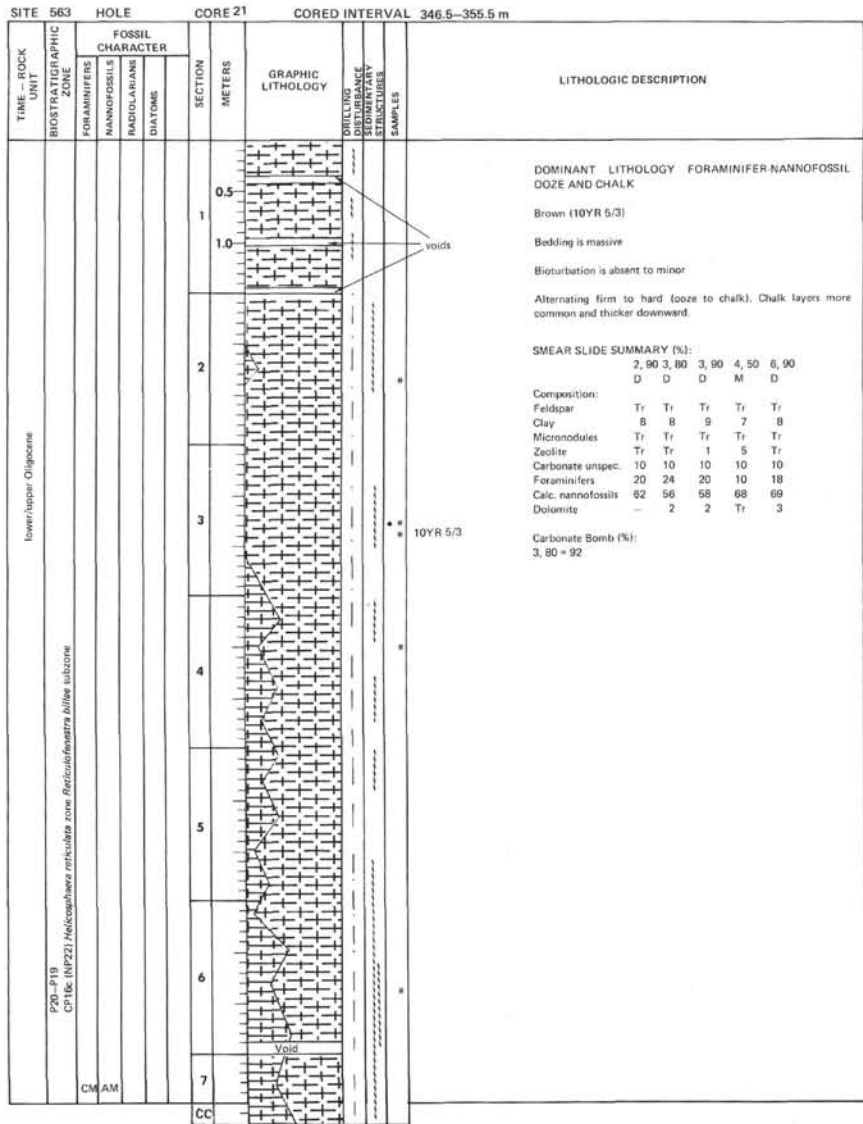


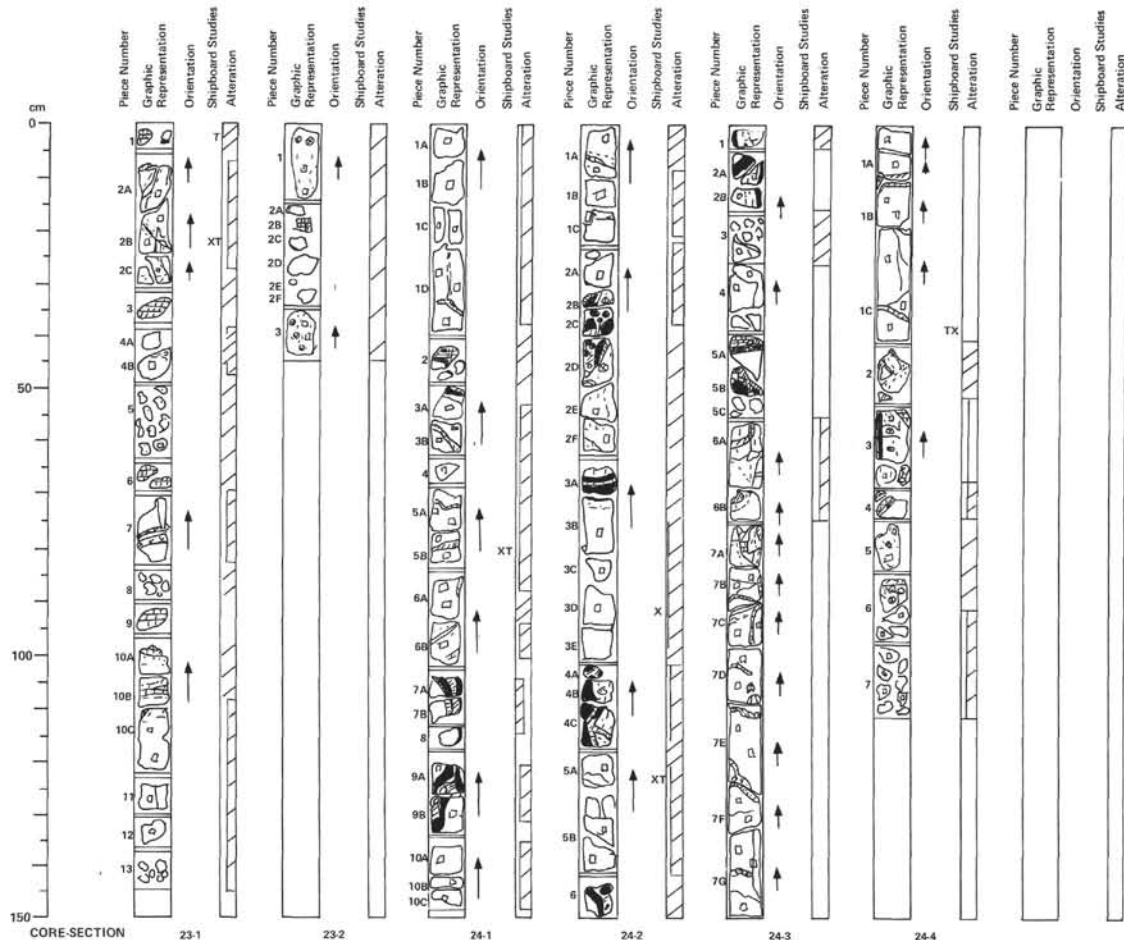
SITE 563 HOLE		CORE 19		CORED INTERVAL 327.5-337.0 m		
TIME - ROCK UNIT	BIOSTRATIGRAPHIC ZONE	FOSSIL CHARACTER		SECTION METERS	GRAPHIC LITHOLOGY	LITHOLOGIC DESCRIPTION
		FORAMINIFERS	NANNOFOSSILS			
		RADIOLARIANS	DIATOMS			
upper Oligocene						
P21	CP18 (NP23) <i>Sphenothus difformis</i> zone			0.5		
				1.0		10YR 5/4
AM	AM			2	OG	
				3		
				CC		

DOMINANT LITHOLOGY FORAMINIFER-NANNOFOSSIL OOZE AND CHALK  
 Yellowish brown (10YR 5/4)  
 Massive bedding  
 Bioturbation is absent to minor  
 Distinct light-colored burrows in Section 3.  
 SMEAR SLIDE SUMMARY (%):  
 1, 80 2, 90  
 D D  
 Composition:  
 Feldspar Tr Tr  
 Clay 10 10  
 Micronodules Tr Tr  
 Zeolite 5 1  
 Carbonate unsp. 10 10  
 Foraminifers 20 25  
 Calc. nannofossils 35 54  
 Dolomite Tr -  
 Carbonate Bomb (%):  
 3, 41 - 89

SITE 563 HOLE		CORE 20		CORED INTERVAL 337.0-346.5 m		
TIME - ROCK UNIT	BIOSTRATIGRAPHIC ZONE	FOSSIL CHARACTER		SECTION METERS	GRAPHIC LITHOLOGY	LITHOLOGIC DESCRIPTION
		FORAMINIFERS	NANNOFOSSILS			
		RADIOLARIANS	DIATOMS			
upper/lower Oligocene						
P21 - P20	CN17 (NP23) <i>Sphenothus praediffertus</i> zone			0.5		
				1.0	Void	
AM	AM			2	Void	
				3	Void	10YR 5/4
				4	Void	
				5	Void	
				6	Void	
				7	Void	
				CC		

DOMINANT LITHOLOGY FORAMINIFER-NANNOFOSSIL OOZE  
 Yellowish brown (10YR 5/4)  
 The entire core is extremely disturbed by drilling. Only very minor bioturbation is occasionally distinguishable.  
 Poor recovery and soupy condition of sediments are probably related to mechanical causes.  
 SMEAR SLIDE SUMMARY (%):  
 1, 55 3, 20 3, 80 7, 30  
 D M D D  
 Composition:  
 Feldspar Tr Tr Tr Tr  
 Clay 5 8 5 5  
 Micronodules Tr Tr Tr Tr  
 Zeolite 3 3 Tr 3  
 Carbonate unsp. 8 5 10 10  
 Foraminifers 15 10 20 10  
 Calc. nannofossils 69 73 85 72  
 Dolomite - Tr - -  
 Carbonate Bomb (%):  
 3, 80 - 95





SITE 563, CORE 23

Depth 364.5–366.5 m

## SECTION 1

## SPARSELY PLAGIOCLASE PHYRIC PILLOW BASALT

Sparsely plagioclase phyric (2–3%) pillow basalt gray (2.5Y N6/0). Microphenocrysts of olivine and/or alteration products thereof are visible. Frequency of olivine is variable, <1–5% in places. Alteration variable as well. Plagioclase phenocrysts are randomly oriented 2–4 mm long and/or rounded 2–5 mm glomerocrysts or laths. Olivine is present <1–2 mm in diameter. Dark orange brown alteration residue is present in most localities rather than fresh olivine itself. Frequency of occurrence is variable.

Sedimentary material (limestone) occurs as interpillow or irregularly shaped veins as indicated. Dendritic pattern of MnO<sub>2</sub> or other oxides is visible in places. Alteration frequently occurs in the basalt adjacent to limestone units. Alteration is moderate overall, higher in places. Highest adjacent to calcite veins and/or limestone units, gray (2.5Y N8/0) to pale brown (10YR 6/2).

Vesicles are scarce, rounded <1–2 mm in diameter and often clay filled. Glass is scarce; Piece 7 has a glassy rind grading into a black (10YR 2/1) aphanitic basalt grading into a very dark gray (10YR 3/1) aphyric to slightly phyric gray (2.5Y N6/0) pillow basalt.

## SECTION 2

## SPARSELY PLAGIOCLASE PHYRIC PILLOW BASALT

0–43 cm: Sparsely plagioclase phyric aphanitic basalt (close to pillow margins). Gray (10YR 5/1) to grayish brown (10YR 6/2) where shown. Plagioclase phenocrysts, prismatic to 1 mm (~1%).

17–19 cm: Limestone as in Section 1 with glass fragment.

SITE 563, CORE 24

Depth 366.5–373.5 m

## SECTION 1

## SPARSELY PLAGIOCLASE PHYRIC PILLOW BASALT

0–50 cm:

Sparsely plagioclase phyric pillow basalt with (micro) phenocrysts of olivine also present 85–150 cm increasing in frequency and size. Gray (1.5YR 5/0) basalt slightly altered along calcite veins and irregular veinlets. Plagioclase crystals 1–5 mm in length and also as rounded laths and/or glomerocrysts 2–4 mm in diameter. Sparsely scattered throughout. No particular concentration anywhere in pillow.

Olivine phenocrysts become visible in hand sample 85–150 cm, in addition to plagioclase. Generally altered to dark orange brown clays (<1–1 mm).

Limestone as well as calcite is present in fractures and on rims of rocks. Alteration is present in rock fractures, adjacent to calcite and limestone veins, slight color change to basalt by yellowish brown (10YR 5/8) hue to gray (2.5Y N5/0) basalt. Also see alteration in gradation to pillow margins (slight increase in gray intensity).

Glass present as rims and interpillow zones. Calcite veins, seem to co-occur with glass (could be incidental, but is noticeable). Slightly reactive with calcite and/or limestone to a palagonite – color calcite.

Sequence of glass to very dark gray (10YR 3/1) aphanitic zone to slightly plagioclase phyric gray (2.5Y N5/0) pillow basalt.

## SECTION 2

## SPARSELY PLAGIOCLASE PHYRIC PILLOW BASALT SEQUENCE AND MINOR GLASS BRECCIA

0–150 cm:

Sparsely plagioclase phyric gray (2.5Y N5/0) basalt with (micro) phenocrysts of olivine as in Section 1. Plagioclase crystals as in Section 1.

Olivine occurrence as in Section 1. Extends throughout core, size increasing to <1–2 mm.

Alteration as in Section 1. In addition, alteration concurrent with variolitic basalt sequence. Variolitic basalt, sequence where noted: glass to black (10YR 2/1) aphanitic basalt to variolite zone of yellow brown (10YR 5/8–10YR 5/6) to gray (2.5Y N5/0) slightly plagioclase phyric.

Glass present where indicated. Co-occurrence with calcite/limestone is enhanced in breccia zone, yet still occurs in whole rock samples.

33–45, 65–67, 100–102, and 143–148 cm: Breccia of glass clasts in a calcite (predominantly) and limestone matrix. Clasts are angular, few mm–few cm in diameter. Slightly palagonite-tinted calcite product rims glass fragments. Some palagonitization of smaller clasts occurs.

## SECTION 3

## SPARSELY PLAGIOCLASE PHYRIC PILLOW BASALT

11–150 cm: Sparsely plagioclase phyric pillow basalt. Fine grained, gray (7.5YR N5). Fairly fresh to moderately altered (light grayish brown – 10YR 6/2) near pillow margins or along fractures. 1–2% plagioclase phenocrysts (2–5 mm), prisms, equant, some with rounded edges (resorbed?). 1–2% plagioclase needles (1–4 mm) randomly oriented. <1% olivine (1–2 mm) mostly altered to red brown clay(?).

0–4 cm: One piece of finer grained aphyric basalt (almost aphanitic) at pillow margin.

6–8 cm: Fresh, black glass clasts with rims altered to reddish yellow (7.5YR 7/6) (generally next to fresher glass) and dark brown (7.5YR 4/4) usually rimming the palagonite, but sometimes also next to glass in calcite-limestone (pinkish gray – 7.5YR 7/2) matrix.

Fractures filled with calcite (XXXX) or pink (7.5YR 8/4) limestone or both mixed together(?) (pinkish gray – 7.5YR 7/2).

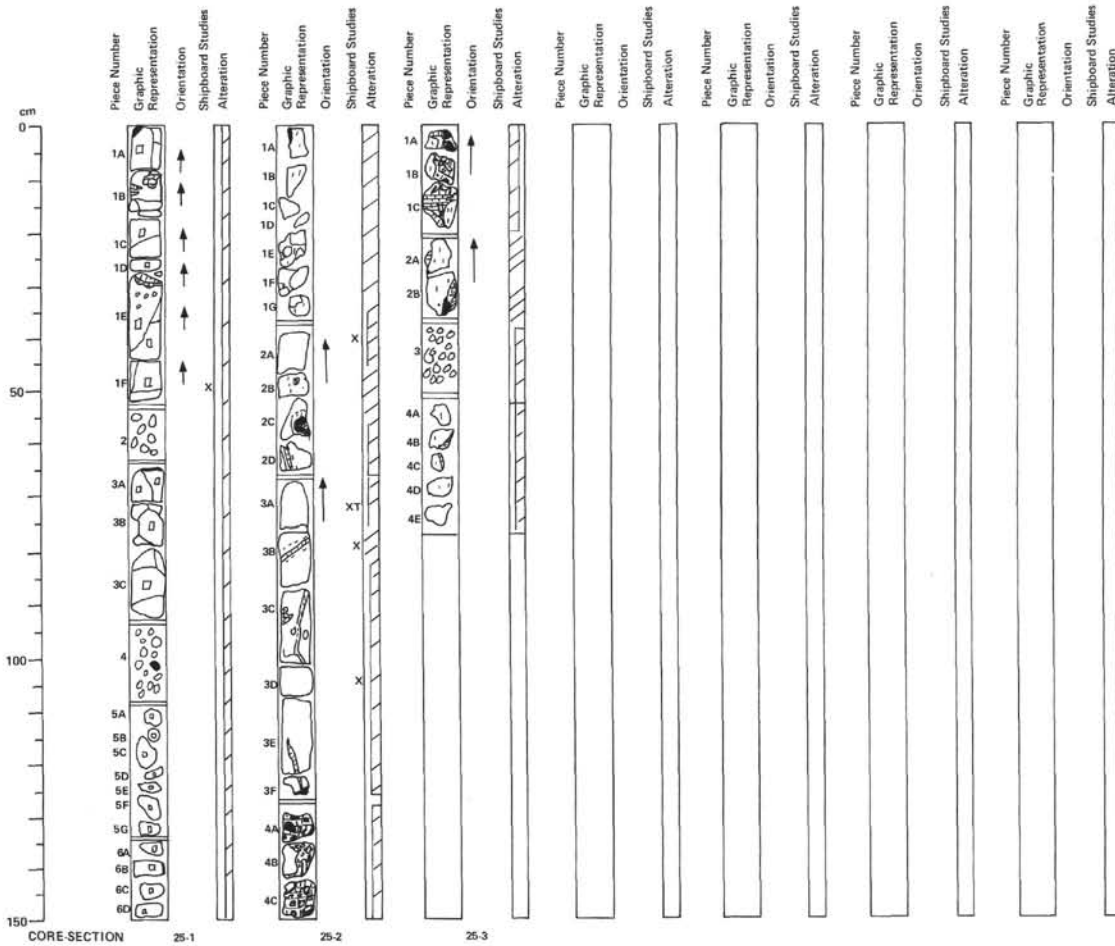
## SECTION 4

## SPARSELY PLAGIOCLASE PHYRIC PILLOW BASALT

0–40 cm: Same as Section 3.

40–150 cm: Very sparse plagioclase phyric to aphyric.

85–86 cm: Basalt with rim of limestone matrix with angular basalt breccia and altered glass clasts (2–4 mm) with outside 4 mm rim of white calcite.



SITE 563, CORE 25

Depth 373.5–382.5 m

## SECTION 1

## SPARSELY PLAGIOCLASE PHYRIC PILLOW BASALT

0–150 cm:

Fine grained, gray (2.5Y N6/0).

&lt;2% plagioclase phenocrysts (1–7 mm); subhedral (slightly resorbed?); partly equant, partly needle shaped.

&lt;1% olivine phenocrysts (&lt;2 mm); eu- and anhedral residues filled with brown clay.

No visible round vesicles.

A few irregular vesicles occur in Piece 1E (30–37 cm). They are coated with calcite cement.

At 0–2, 64–65, 100–102, and 138–142 cm occur fresh black glass rinds.

Limestone occurs at 8–13 cm, yellowish red (5YR 4/6) and at 28–40 cm, pink (5YR 7/3), partly as vein filling.

The boundary between basalt and limestone is often very irregular (lobes).

## SECTION 2

## SPARSELY PLAGIOCLASE PHYRIC PILLOW BASALT

Fine grained gray (2.5Y N6/0) sparsely plagioclase phyric pillow basalt with (micro) phenocrysts of dark orange brown alteration product of olivine.

1–2% plagioclase phenocrysts 1–5 mm needle form or 2–5 mm diameter rounded aggregates and/or glomerocrysts.

~1% olivine phenocrysts &lt;2 mm in diameter euhedral to anhedral residual alteration residue dark orange brown in color. Sparsely scattered as well.

Vesicles rare to absent; only present near glass and only visible with hand lens.

Alteration to light gray (10YR 6/0) in patches with fresh "cores" of gray (2.5Y N6/0) basalt. Mainly occurs in Pieces 1A–G. Alteration present adjacent to rock fractures, calcite veins and limestone patches; to light gray (10YR 6/0) through light brownish gray (10YR 6/2).

Variscitic zone where noted. Slight color change with addition of yellowish brown (10YR 5/8) hue to gray basalt. Slight change in gray intensity. Glass present as indicated.

127–150 cm: Glass breccia in a calcite and limestone matrix. Clasts are angular, few mm to few cm in diameter. Some palagonitization of glass clasts occurs, as well as a palagonite-lined sedimentary product between clasts and matrix.

## SECTION 3

## SPARSELY PLAGIOCLASE PHYRIC PILLOW BASALT AND GLASS BRECCIA

Fine grained gray (2.5Y N6/0) to light gray (10YR 6/0) sparsely plagioclase phyric pillow basalt as in Sections 1 and 2. Slightly more altered in glassy zones than in Section 2. Gravel pieces (Piece 3) more of a light brownish gray (10YR 6/2), possible indicating a higher degree of alteration than in above sections. (Micro) phenocrysts of dark orange brown alteration residue of olivine.

Plagioclase phenocrysts as in Section 2; rounded 1–3\* mm in diameter.

Olivine as in Section 2.

Vesicles absent.

Alteration as in Section 2 and as indicated. Light gray (10YR 6/0) to light brownish gray (10YR 6/2) alteration of basalts.

Glass as indicated.

0–18 cm: Glass breccia with calcite and limestone matrix. Angular clasts, edges palagonitized. Few large (few cm) fine grained basalt clasts, light brownish gray (10YR 6/2) and altered as indicated. Palagonite.

